AD-A067 338 UNITED TECHNOLOGIES CORP STRATFORD CT SIKORSKY AIRCR--ETC F/G 1/3
AEROELASTICALLY CONFORMABLE ROTOR MISSION ANALYSIS.(U)
MAR 79 R H BLACKWELL, S J CASSARINO DAAJ02-77-C-0041
UNCLASSIFIED SER-510017 USARTL-TR-79-5 NL

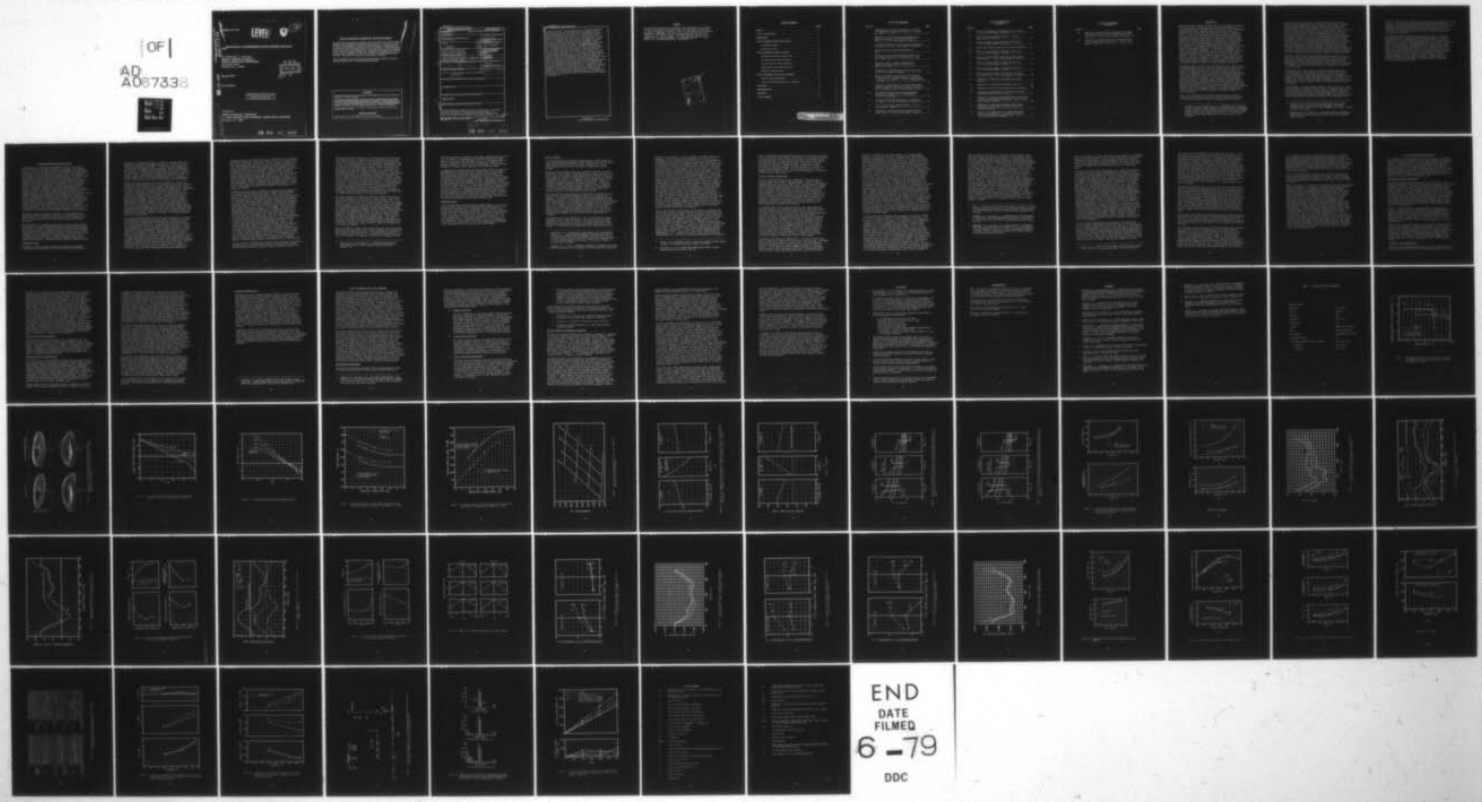

END
DATE FILMED
6-79
DDC

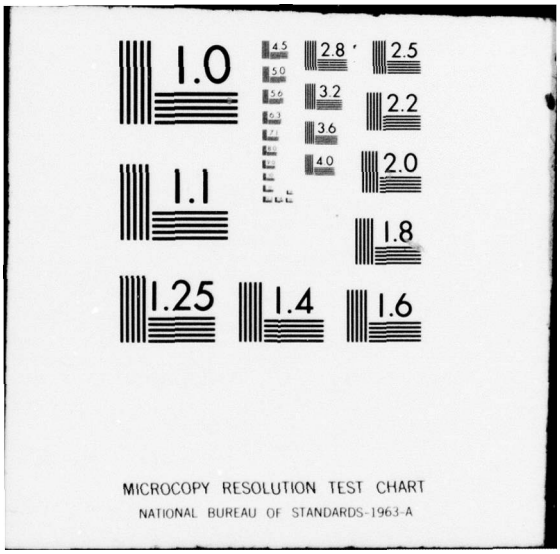
1.0
1.1
1.25
1.4
1.6
1.8
2.0
2.2
2.5
2.8
3.2
3.6
4.0
4.5
5.0
5.6
6.3
MICROCOPY RESOLUTION TEST CHART
NATIONAL BUREAU OF STANDARDS-1963-A

USARTL-TR-79-5

LEVEL II

12

AD A067338

AEROELASTICALLY CONFORMABLE ROTOR MISSION ANALYSIS

R. H. Blackwell, S. J. Cassarino
SIKORSKY AIRCRAFT DIVISION OF
UNITED TECHNOLOGIES CORPORATION
North Main Street
Stratford, Conn. 06602

March 1979

Final Report

Prepared for

APPLIED TECHNOLOGY LABORATORY
U. S. ARMY RESEARCH AND TECHNOLOGY LABORATORIES (AVRADCOM)
Fort Eustis, Va. 23604

APPLIED TECHNOLOGY LABORATORY POSITION STATEMENT

An analytic study was performed by Sikorsky Aircraft to identify the merits and overall suitability of the Aeroelastically Conformable Rotor (ACR) for a typical Army mission. This task was accomplished by establishing the analytic design of a practical ACR that best satisfies the performance requirements of the UTTAS mission. UTTAS performance, vibration, rotor loads, and handling qualities characteristics were computed and compared for the ACR and the standard UH-60A rotor. Manufacturing implications and risk areas including maneuver capability and sensitivity of vibration to blade dissimilarities were examined. The results of this program are documented in this report.

The ATL technical monitor for this program was Mr. Patrick A. Cancro of the Aeromechanics Technical Area, Aeronautical Technology Division.

Unclassified

SECURITY CLASSIFICATION OF THIS PAGE (When Data Entered)

REPORT DOCUMENTATION PAGE

READ INSTRUCTIONS BEFORE COMPLETING FORM

1. REPORT NUMBER: USARTL-TR-79-5	2. GOVT ACCESSION NO.
3. RECIPIENT'S CATALOG NUMBER	
4. TITLE (and Subtitle): AEROELASTICALLY CONFORMABLE ROTOR MISSION ANALYSIS.	5. TYPE OF REPORT & PERIOD COVERED: Technical Report
6. PERFORMING ORG. REPORT NUMBER: SER-510017	
7. AUTHOR(s): R. H. Blackwell, S. J. Cassarino	8. CONTRACT OR GRANT NUMBER(s): DAAJ02-77-C-0041
9. PERFORMING ORGANIZATION NAME AND ADDRESS: Sikorsky Aircraft Division of United Technologies Corporation, Stratford, Conn. 06602	10. PROGRAM ELEMENT, PROJECT, TASK AREA & WORK UNIT NUMBERS: 62209A; 1L262209AH76; 00 205 EK
11. CONTROLLING OFFICE NAME AND ADDRESS: Applied Technology Laboratory, U.S. Army Research & Technology Laboratories (AVRADCOM), Fort Eustis, Virginia 23604	12. REPORT DATE: March 1979
	13. NUMBER OF PAGES: 74
14. MONITORING AGENCY NAME & ADDRESS (if different from Controlling Office): Robert H. Blackwell, Sebastian J. Cassarino	15. SECURITY CLASS. (of this report): Unclassified
	15a. DECLASSIFICATION/DOWNGRADING SCHEDULE

16. DISTRIBUTION STATEMENT (of this Report)

Approved for public release; distribution unlimited.

Final rept., 75p.

17. DISTRIBUTION STATEMENT (of the abstract entered in Block 20, if different from Report)

18. SUPPLEMENTARY NOTES

19. KEY WORDS (Continue on reverse side if necessary and identify by block number)

Helicopter Rotor
Dynamic Twist

20. ABSTRACT (Continue on reverse side if necessary and identify by block number)

An analytic study was conducted to assess the suitability of a conformable rotor for satisfying the requirements of a typical Army mission. A conformable rotor blade is a blade designed to produce changes in blade twist, with azimuth and flight condition, which improve performance

over

DD FORM 1 JAN 73 1473 EDITION OF 1 NOV 65 IS OBSOLETE

Unclassified

SECURITY CLASSIFICATION OF THIS PAGE (When Data Entered)

and reduce rotor loads. This study quantified the performance advantages and rotor system load reductions possible with a conformable rotor by designing blades suited for the UH-60A mission and comparing calculated rotor behavior with that of the UH-60A rotor. Relative to the UH-60A design, the conformable blade employs a four-to-one reduction in torsional stiffness over the outer half of the blade, a reduction in built-in twist from -16 to -12 degrees, an increase from 20 to 30 degrees in tip sweep and reflex tab deflection inboard of the 80-percent radial position. This design produces elastic response which increases twist in hover and reduces advancing blade twist in forward flight. At UH-60A design point conditions, the analysis projects a 2-percent increase in cruise L/D, a 1.2-percent increase in hover figure of merit and a 210-ft/minute increase in vertical rate of climb capability. Modest reductions in blade stress and control loads were provided by the conformable rotor for cruise at design gross weight. This is in contrast to the usual increase in forward flight blade loads associated with conventional rotors achieving high hover figures of merit through increases in built-in blade twist. Analysis projects that the conformable rotor design would degrade performance slightly at alternate gross weight and maneuvering conditions where retreating blade stall is more important than advancing blade compressibility losses. Brief examination showed little effect of the conformable rotor on aircraft handling qualities characteristics or on sensitivity of non n/rev aircraft vibration to blade dissimilarities. Material and fabrication requirements imposed by the conformable rotor were reviewed, and practical techniques for providing required torsional stiffness reductions are suggested. Projected performance improvements due to the conformable rotor were sensitive to modeling of the detailed aerodynamics of the advancing blade tip, and it is important that the accuracy of the analysis be confirmed through model tests.

PREFACE

The work reported herein was performed by the Sikorsky Aircraft Division of United Technologies Corporation under Contract DAAJ02-77-C-0041 for the Applied Technology Laboratory of the U.S. Army Research and Technology Laboratories (AVRADCOM). The work was performed under the technical cognizance of Mr. Patrick Cancro. Personnel involved directly in the program were Mr. Robert Blackwell, Mr. Sebastian Cassarino, Mr. Robert Moffitt, Mr. Timothy Krauss and Mr. James Howlett.

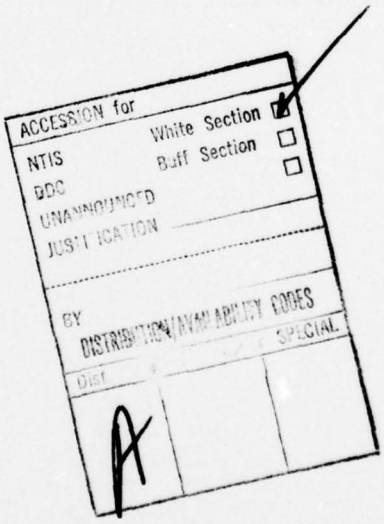

TABLE OF CONTENTS

LIST OF ILLUSTRATIONS

LIST OF ILLUSTRATIONS
(continued)

LIST OF ILLUSTRATIONS
(continued)

INTRODUCTION

Helicopter evolution depends on continuing effort to improve all aspects of rotor behavior. Reduced vibration, noise and vulnerability and increased aerodynamic efficiency will all be required in next-generation rotary-wing aircraft. Improving rotor efficiency to reduce fuel consumption is a particularly desirable goal in light of rising fuel costs. A number of investigators have explored means of improving helicopter main rotor efficiency through the use of advanced airfoils, tip geometry and twist distributions. Considerable effort has been expended in devising systems which vary blade twist or higher harmonic control input with flight condition to further optimize performance. An area which has received attention within the last few years is the possibility of designing blades which produce an azimuthal variation in elastic twist that improves such attributes as vibration, blade loads or aerodynamic performance. In the area of performance it is clear that the twist selected for a given aircraft mission is typically a compromise between that desired for various high and low speed segments. Moreover, there is little reason to expect that the twist which is optimal at, for instance, 90 degrees of rotor azimuth is also optimal at 270 degrees azimuth. The effects of blade dynamic twist on performance must be understood so that designers can take advantage of potential beneficial effects or minimize detrimental effects.

The immediate goal of research in this area has been to quantify the performance gains and rotor system load reductions which can be achieved through variation of elastic twist with azimuth and to define the aeroelastic blade design features required to produce desired twist. A more far-reaching goal is to provide generally improved understanding of torsional response so that design criteria reflecting effects of elastic twist can be formulated. In the past only crude guidelines have been available to constrain blade stiffness or pitching moment generating capacity. The design process proceeds based on scaling of past successful configurations. This procedure obviously becomes less effective as changes in rotor type, airfoil or material are approached. Improved design criteria in conjunction with improved aeroelastic modeling capability will allow designers to specify the blade properties and elastic response which produce the greatest possible advantage for a given application.

Study of the potential role of blade torsional response effects in improving rotor attributes began with the work described in Reference 1. That study explored the effects of changes in blade torsional

---

1. Blackwell, R.H., and Commerford, G.L., INVESTIGATION OF THE EFFECTS OF BLADE STRUCTURAL DESIGN PARAMETERS ON HELICOPTER STALL BOUNDARIES, Sikorsky Aircraft Division, United Technologies Corporation; USAAMRDL Technical Report 74-25, Eustis Directorate, U.S. Army Air Mobility Research and Development Laboratory, Fort Eustis, VA, May 1974, AD 784594.

properties on flight envelopes. It was shown that reducing blade stiffness reduced envelope-limiting vibratory control loads. A number of other design changes which reduced blade or control system loads were also identified. The Compliant Rotor Study conducted under Contract DAAJ02-76-C-0003 and reported on in References 2 and 3 defined the elastic twist required to improve various aspects of rotor behavior. Of the many effects which could be accomplished, it was determined that the most valuable in terms of providing expanded flight capability and reduced operating cost would be the improvement of forward flight performance. Moreover, results suggested that dedication of elastic twisting reponse to the improvement of performance, because the response acts to produce a more efficient azimuthal distribution of airloads, achieved performance gains which could not be achieved through other aerodynamic means such as planform changes or application of advanced airfoils. Predicted performance gains were not large unless the baseline rotor was stalled, but there were definite trends for improved performance with one/rev dynamic twist which tended to untwist the advancing blade.

Two needs became evident at the conclusion of that program. First, there was a need to test torsionally conformable rotor blades to quantify analytically projected trends and provide a data base for upgrading aeroelastic analyses. This need resulted in sponsorship by the U.S. Army Research and Technology Laboratories of two so-called Aeroelastically Conformable Rotor (ACR) wind tunnel model test programs to be performed in the near future.

Second, there was a need to explore the overall effectiveness of a conformable rotor in satisfying a typical set of mission objectives. A clear statement of the advantages and the possible shortcomings associated with rotor blades employing passive control of blade torsional response was needed. Modest performance advantages, if achieved at minimal cost, should be pursued; however, performance gains which significantly increase cost or compromise other aircraft attributes may not be justifiable.

The requirement for improved understanding in this area led to the work described below. The objectives were, first, to translate design features producing trends of improved rotor performance or reduced blade loads into a rotor system providing significant advantages with respect to a conventional rotor and, second, to examine other rotor attributes which might be unfavorably affected by application of the conformable rotor

---

2. Blackwell, R.H., INVESTIGATION OF THE COMPLIANT ROTOR CONCEPT, Sikorsky Aircraft Division, United Technologies Corporation, USAAMRDL TR 77-7, Eustis Directorate, USAAMRDL, Fort Eustis, Virginia, June 1977, AD A042338.

3. Blackwell, R.H., and Merkley, D.J. THE AEROELASTICALLY CONFORMABLE ROTOR CONCEPT, American Helicopter Society, 34th Annual National Forum, May 1978.

concept. These attribute risk areas include rotor design complexity and cost, sensitivity of vibration to blade-to-blade dissimilarities, handling qualities, manuever capability and operation at off-design flight conditions. Fundamental limitations associated with a conformable rotor in any of these areas must be identified and subjected to further scrutiny. If any such flaws are present and cannot be overcome, performance advantages of an ACR would be immaterial.

The approach adopted in pursuit of these objectives was to expand upon the conformable rotor design work described in Reference 2 to evolve a design suitable for the UH-60A mission and then to compare calculated behavior for the baseline UH-60A and conformable rotor designs. Comparisons were made in the areas of rotor performance, rotor and control system loads, aircraft vibration, handling qualities and manufacturing requirements. The UH-60A mission was selected for this comparison because the UH-60A rotor system represents state-of-the-art technology and because there is readily available test data for evaluation of analytic results. It is expected that trends in such areas as performance, vibration or handling qualities would be similar for other aircraft missions, although magnitudes of the various advantages or disadvantages with respect to baseline designs would be strongly dependent on detailed blade and mission characteristics.

UH-60A CONFORMABLE ROTOR DESIGN STUDY

A design study was conducted in an attempt to define a conformable rotor configuration which would improve the performance of the UH-60A aircraft. All other aircraft systems such as engines, transmission and fuselage geometry were maintained in the UH-60A Black Hawk configuration. The specific measure of improved performance used was the savings in fuel required to perform the primary UH-60A mission. The primary mission requirements include a 2.3-hour endurance mission made up of short warmup and hover segments and cruise at 145 knots and 16,450 lbs gross weight at conditions of 4000-ft pressure altitude and 95° Fahrenheit. A 30-minute fuel reserve is required. The aircraft is also required to perform a 480-ft/min vertical rate of climb using not more than 95 percent of installed intermediate power. Under the guidelines of the contract, increases in airspeed, payload or climb rate beyond the UH-60A specifications were not sought. Other potential objectives such as reduced vibration, rotor loads and control system loads were not specifically addressed although these parameters were monitored in evolving the design. Improvement of Black Hawk cruise performance was expected to be an ambitious goal since at cruise the rotor is free of advancing blade drag divergence effects or retreating blade stall. Results of Reference 2 showed that performance advantages to be obtained by controlling dynamic twist became most significant for high speed or marginally stalled conditions. The behavior of the rotor at other flight conditions was examined only briefly in selecting the design but is evaluated thoroughly in the section entitled "UH-60A Conformable Rotor Evaluation".

The design study was conducted in two parts. The first phase was a preliminary design study which selected (a) the combination of rotor radius, chord and tip speed most compatible with the conformable rotor and (b) the mean and time-varying blade twist required to optimize performance.

The second phase of the design procedure was a structural design study performed with the Y200 Normal Modes Blade Aeroelastic Response Analysis which sought to produce the desired twisting by changing such parameters as torsional stiffness, tip geometry, built-in twist and airfoil camber. As described below, the preliminary and detailed design analyses include different rotor aerodynamic and inflow models. It was found that these differences led to predictions of larger performance gains in the preliminary design phase than were finally determined using the more complete Y200 analysis. Preliminary design results are documented below.

PRELIMINARY DESIGN

Preliminary aircraft design is normally accomplished by performing trending studies which relate aircraft cost, weight and performance to

variations in aircraft subsystems. Iteration is performed until the combination of parameters providing the most cost effective solution to mission requirements is determined. In selecting rotor geometry, the iteration process normally includes resizing of engines, transmission and airframe. For example, if a more efficient rotor can be devised, it may be possible to satisfy mission payload requirements with a smaller (lighter) rotor. Reduced rotor size may permit reductions in tail cone length, antitorque requirements, transmission capacity or control system strength, all of which reduce empty weight. The reduced weight, in turn, permits further reduction in rotor power and fuel consumed.

Because the present study was not aimed at designing an aircraft but assessing the potential and risks of a particular rotor concept, iteration between rotor size, aircraft size, engines, transmissions, etc, was not performed. Small changes in rotor geometry were examined while maintaining basic UH-60A airframe, transmission and engine characteristics. Also, in order to permit direct evaluation of rotor twisting effects, the airfoils of the UH-60A blade were assumed. The UH-60A blade has a 9.5-percent-thick cambered airfoil (SC 1095). Between the 50- and 80-percent radial stations, leading edge camber is increased to provide higher $c_{l_{max}}$ (SC 1095R8). For reference, Table 1 lists the UH-60A Black Hawk rotor design parameters. The Sikorsky Airload Optimization Analysis and Circulation Coupled Hover Analysis Program (CCHAP) were used to project the gains in cruise and hover performance which could be achieved by controlling dynamic twist and to define the required twisting. The Helicopter Design Model (HDM) was then used to determine whether the improvements in rotor efficiency provided the opportunity for beneficial changes in rotor radius, solidity or tip speed. The savings in mission fuel was then calculated.

The Airload Optimization Analysis is described in Reference 2. Basically this program uses variational calculus criteria to determine the radial distribution of airloading which minimizes power losses due to drag while maintaining required lift. The program then determines the angle of attack distribution required to achieve optimal performance. Based on the ideal angle of attack distribution, control inputs and an assumed inflow pattern, the program determines the timewise variation in twist required for optimal performance. The optimization program can be run using either a uniform or variable inflow representation. The ideal angle of attack pattern is the same in either case, but the twist required to achieve it depends upon the inflow. Past results (Reference 2) had not shown significant differences between the ideal dynamic twist patterns predicted using uniform and variable inflow. This result and a significant savings in computer time led to use of the uniform inflow model. The program was exercised at the Black Hawk cruise speed for a range of rotor lift values. Because results of Reference 2 had suggested that the UH-60A rotor might derive advantage from reduced tip speed, the

analysis was run at the nominal 725-ft/sec tip speed and at a 5% reduced tip speed of 690 ft/sec. Results are shown in Figure 1 for baseline and ideal rotors. Reduction in tip speed by itself is shown to improve rotor L/D by approximately 10 percent up to about 15,000 lbs gross weight, at which point retreating blade stall deteriorates the performance of the reduced tip speed rotor. At design gross weight (16,450 lb), performance is degraded with the reduced tip speed. Producing ideal twisting to minimize power results in a 10-percent increase in L/D at either tip speed. Figure 2 presents surface plot comparisons of angle of attack and airload distributions at design weight and tip speed. As shown, the ideal rotor avoids negative angles of attack and negative loading at the tip of the advancing blade and high angles of attack at the tip of the retreating blade. Figure 3 illustrates the azimuthal variation in twist for the ideal rotor at this condition, assuming uniform inflow. A mean twist of approximately -16 degrees and a one-per-rev variation of $\pm$ 7 degrees are required.

The CCHAP was used to assess the impact of blade twist on performance in hover and at the 480-ft/min vertical rate of climb condition required for the Black Hawk at design gross weight. CCHAP, as described in Reference 2, performs a coupled calculation of the rotor load distribution and the contracted rotor wake geometry. Performance predictions within 2% of measured values are typically obtained. Power was calculated for the hover and climb conditions as a function of blade twist to determine an optimal value. The Black Hawk airfoils and tip sweep were assumed. Linear twist values or -12, -16, -20 and -24 degrees and the nonlinear twist distributions shown in Figure 4 were examined. Nonlinear twist distributions of the form illustrated in the figure have been shown to improve hover performance by improving the induced efficiency of the lift distribution in the region of the blade which passes over the tip vortex trailed by the preceding blade. Hover and climb power required are shown in Figure 5 for the two twist families. For the same equivalent twist, the nonlinear twist distribution gives consistently improved performance. The optimal twist is approximately -24 degrees. Twist increases above this value provide little additional benefit. The baseline Black Hawk twist, including elastic windup, and required power values are included in Figure 5. Relative to the Black Hawk rotor, increasing the total twist to approximately -24 degrees results in a 30-hp savings (1.7% figure of merit increase) in hover and a 45-hp savings (2.4% figure of merit increase) at the climb condition. Figure 6 shows the variation with twist angle of the rate of climb achievable using the power calculated for the baseline UH-60A rotor at the 480-ft/minute vertical climb condition. Relative to the UH-60A rotor, increasing twist to -24 degrees would provide a 260-ft/minute rate of climb increase.

The HDM was used to translate the cruise and hover performance improvements anticipated for the ACR into UH-60A mission fuel savings and to define trends of mission fuel with changes in radius, chord and tip speed. The

HDM program described in Reference 4 uses measured and calculated data defining the effects of changes in aircraft configuration on aircraft cost, weight or mission fuel to aid the designer in evolving optimal designs. In examining the ACR, it was assumed that conventional trends of power and fuel consumption with geometry change would apply but that the control of blade twisting would provide cruise L/D and hover FM values which were uniformly higher than those of a conventional rotor. The program determined the savings in mission fuel which would result from improvements in rotor efficiency and basic changes in rotor geometry. Aircraft drag, engine fuel consumption, transmission losses and tail rotor efficiency measured on the UH-60A aircraft were assumed. Figure 7 relates changes in rotor efficiency (forward flight L/D and hover figure of merit) to mission fuel and shows little effect of figure of merit on mission fuel, reflecting the short hover segment of the assumed mission (5 minutes). The 10-percent improvement in cruise L/D predicted with the Airload Optimization Analysis for the ACR would produce a fuel savings of approximately 90 lbs or approximately 4.5% of the total. Because of the large parasite drag of the UH-60A utility airframe, the percentage savings in fuel resulting from increases in rotor efficiency are smaller than they would be on a lower drag aircraft.

The second application of HDM was to determine whether the increase in efficiency assumed for the ACR leads to a set of radius, chord and tip speed values different from those of the baseline UH-60A rotor. A 10% increase in cruise L/D and a 2% increase in figure of merit were assumed. Because resizing of the aircraft was not being considered, gross changes in rotor geometry and tip speed were not examined. Changes in radius and tip speed which would be possible without changing fuselage length or transmission design were examined. Vertical rate of climb and mission fuel trends were examined for radius, chord and tip speed variations. CCHAP was first used to define effects of geometry changes on climb capability, assuming -24 degrees of nonlinear twist. Figure 8a shows that the power required to perform the 480-ft/minute climb can be reduced by increased radius and decreased tip speed or decreased chord. Alternately the climb rate could be increased using available power, as illustrated in Figure 8b. Again, increased radius and decreased chord or tip speed are desired.

Effects of geometry changes on mission fuel were then explored with HDM, and conflicting trends were found. Figure 9 suggests that increased tip speed and chord reduce mission fuel. Increasing radius, predicted to have a slightly beneficial effect, is not practical based on main rotor/ tail rotor clearance. The effects on mission fuel of changes in blade

---

4. Kefford, N.F.K., and Campbell, B., SIKORSKY HELICOPTER DESIGN MODEL USER'S GUIDE, Sikorsky Engineering Report SER-50851, November 1973.

weight are included in the model. Blade weight trending was based on $W_b \propto R\, C^{1.25}\, (\Omega R)^{1.4}$. The combinations of increased chord and tip speed which still meet the climb requirement (because of the higher figure of merit to be provided by the ACR) were calculated with CCHAP and are included in Figure 9. Based on these considerations, the optimal design includes a 3% increase in tip speed and a 5% increase in chord.

In preparation for conducting the structural design study, the trends of performance with chord and tip speed predicted with the Y200 program were checked at the Black Hawk cruise condition, assuming that the prescribed one-per-rev lateral twisting was achieved. In this case cruise power was predicted to be insensitive to the chord change proposed and adversely affected by increased tip speed. Examination of test data at approximately the cruise guarantee condition did indicate slightly reduced cruise power with increased tip speed, although there was considerable scatter among the data. It is not clear whether the trend predicted by Y200 is correct. The effect of tip speed on total power depends upon the relative severity of advancing blade compressibility effects and retreating blade stall. Increased tip speed relieves retreating blade stall but aggravates advancing blade drag divergence effects. Y200 may be overpredicting the relative importance of advancing blade drag. In any case it was decided to conduct the structural design study using the tip speed and chord values of the baseline UH-60A rotor.

STRUCTURAL DESIGN

The Y200 Normal Modes Blade Aeroelastic Response Analysis was used in an attempt to define sets of blade parameters which produce elastic twist that enhances performance at the Black Hawk cruise condition. Non-uniform rotor inflow was used consistently. Results of the preliminary design study which determined optimal twist with uniform inflow were to be used as a guide. The design effort was intended to be limited in scope, relying heavily on the results described in Reference 2. The only additional area to be addressed was the effect of tip speed and chord variations. Also, there was a desire to confirm the Reference 2 trends with the current version of the Y200 program which has undergone several improvements since the earlier work was performed.

Analytic Methods

The Normal Modes Blade Aeroelastic Response Analysis (Y200 Program) and the Prescribed Wake Inflow Analysis (F389 Program) delivered to the Army under Contract DAAJ02-77-C-0047 were used. References 2, 5 and 6 provide detailed description of the analytic methods used in these programs.

Briefly, the Y200 program solves the coupled blade equations of motion by expanding them in terms of uncoupled flatwise, edgewise and torsional modes. Up to five flatwise, three edgewise and two torsional modes can be considered in addition to rigid body flap and lag modes. The present study used three flatwise, one edgewise and two torsional modes. Blade aerodynamics are based on a lifting line representation. Steady or unsteady aerodynamic modeling is available (see below). The analysis includes multiblade capability and the modeling of either a rigid body airframe or a grounded flexible support. Except for the determination of rotor stability derivatives described later in this report, the analysis was used in the single blade (fixed hub) mode.

The Prescribed Wake Inflow Analysis determines the distribution of rotor inflow based on a prescribed geometric pattern of the trailing wake elements. In this study the classical nondistorted skewed helical wake structure was assumed. Blade loading and circulation distributions are calculated based on section operating conditions and section lift coefficient data. The strengths of the trailing vortex elements are then determined, based on the spanwise variation in bound circulation. The contribution of each of the trailing vortex segments to induced velocity at each blade position is calculated, using the Biot-Savart law. The solution proceeds until the bound circulation distribution, the strength of the trailing vortex elements, and the induced velocity distribution are compatible.

The Compliant Rotor Study (Reference 2) used a two-dimensional unsteady aerodynamic model. Radial flow effects, including relief of tip Mach number due to sweep, were not treated. The study used variable inflow distributions calculated with the Prescribed Wake Inflow Analysis (F389 program). In approaching the present study, three changes were made in

---

5. Arcidiacono, P.J., PREDICTION OF ROTOR INSTABILITY AT HIGH FORWARD SPEEDS, VOL. I, STEADY FLIGHT DIFFERENTIAL EQUATIONS OF MOTION FOR A FLEXIBLE HELICOPTER BLADE WITH CHORDWISE MASS UNBALANCE, Sikorsky Aircraft Division, United Technologies Corporation; USAAVLABS 68-18A, U.S. Army Aviation Materiel Laboratories, Fort Eustis, Virginia, February 1969, AD 685860.

6. Langdrebe, A.J., et al., AERODYNAMIC TECHNOLOGY FOR ADVANCED ROTORCRAFT, American Helicopter Society, Symposium on Rotor Technology, August 1976.

modeling rotor aerodynamics. First, unsteady aerodynamic effects were neglected. This decision was based primarily on the fact that the conformable rotor at cruise will not be stalled. The second change was to implement the steady three-dimensional aerodynamic model used in the Sikorsky Generalized Rotor Performance Program. This aerodynamic model is essentially the same as that documented in Reference 7. The model treats the details of blade element lift and drag characteristics more rigorously than the two-dimensional model and has been shown to improve correlation between measured and predicted rotor performance. Accurate modeling of radial flow effects is especially important for swept tips which are a powerful source of blade pitching moment for a conformable rotor. The third area to be modified was the coupling between the Y200 program and the inflow analysis. These two programs solve for blade response and rotor inflow on an iterative basis. Blade pitch angles and response quantities needed to calculate noninduced velocity components are transferred from Y200 to the inflow analysis. The inflow program then computes and feeds to Y200 the distribution of induced velocities. The process continues until angle of attack patterns for consecutive runs converge. Until recently the inflow analysis included blade flapping and elastic pitching in the calculation of circulation but did not treat blade bending motion. This assumption caused the loading distribution used by the wake analysis to be inconsistent with that used in Y200. Local angle of attack discrepancies between the programs of as much as 3 degrees resulted. Angle of attack differences were most prominent on the retreating blade where relative velocities are low and at the tip of the advancing blade where plunging rates are significant. The Y200 program was modified to provide required data to the inflow program, and this discrepancy was eliminated.

Prior to exercising the Y200 program for the study of conformable rotor effects, the correlation between measured and predicted performance and rotor system loads was assessed. Figure 10 compares results calculated with uniform and variable inflow with YUH-60A test data from Reference 8. Analytic results were calculated at the atmospheric conditions of the cruise guarantee point (4000 ft pressure altitude and 95° F). Test data were acquired at 2000 ft hp and 65° F. Measured performance data were corrected to the 4000 ft/95° F condition. Rotor system load data were not corrected to the guarantee condition, but differences are expected to be very small. Rotor performance is reliably predicted when variable inflow effects are included. Correlation of blade bending moment and pushrod loads, however, is only fair. Each load is underpredicted by approximately 2 to 1. Inclusion of variable inflow reduces predicted flatwise moments as a result of decreased tip downloading on the advancing

---

7. Harris, F.D., PRELIMINARY STUDY OF RADIAL FLOW EFFECTS ON ROTOR BLADES, Journal of the American Helicopter Society, July 1966.

8. Ericsion, W., et al., FLIGHT LOADS SURVEY TEST REPORT, Sikorsky Engineering Report SER-70406, May 1976.

blade. Correlation was generally less satisfactory than has been achieved in the past on other blade designs. References 1 and 2 present correlation of Y200 predictions with test data from low twist CH-53A blades and high twist CH-53D blades. Flatwise moments and pushrod loads were generally increased when variable inflow was included. Predictions 20 percent less than test data were typically obtained. Reasons for the less satisfactory correlation achieved on the UH-60A blade were sought, but no clear explanations were found. The differences may result from changes in the treatment of the wake or from shortcomings in the modeling of high nonlinear twist blades.

Effects of Camber and Tip Sweep

Results of the Compliant Rotor Study (Reference 2) had shown that tip sweep and camber exert powerful twisting moments. Sweep and noseup pitching moment can be used to untwist the advancing blade, which generally improves performance and reduces blade loads. It was decided to examine effects of these parameters with the updated Y200 program at the UH-60A cruise condition. Objectives were to verify the twisting produced by the two parameters and to determine the effects of that twisting on rotor performance. Results described below confirm the effectiveness of airfoil camber for producing one-per-rev lateral elastic twisting. As a result of modifications to the Y200 aerodynamic model, tip sweep is not predicted to have as strong an effect on one-per-rev twisting as was predicted in Reference 2. Moreover, at the cruise condition, rotor performance calculated using nonuniform inflow was determined to be fairly insensitive to elastic twist changes.

In examining camber and tip sweep variations, other blade parameters were held fixed at values selected in the Compliant Rotor Study. Blade torsional stiffness was reduced by a factor of four outboard of the 50-percent radial position. This stiffness reduction permits achievement of desired levels of torsional response with realistic amounts of camber or tip sweep. The stiffness reduction was made in the outboard section of the blade to enhance outboard elastic twisting desired for improved performance (see Figure 2). To further concentrate twisting along the blade, the control system stiffness was assumed to be ten times higher than that of the baseline UH-60A rotor. The resulting torsional frequency of the conformable blade was 3.80P as opposed to 4.2P for the baseline UH-60A blade. Past results indicated that for the anticipated levels of steady and one-per-rev elastic response, a built-in twist value of approximately - 12 degrees gave the best overall performance. Minus 11.6 degrees of nonlinear twist having a distribution similar to those shown in Figure 3 was assumed.

Variations in tip sweep were examined first. The baseline UH-60A blade employs 20 degrees of sweep at the 93.5-percent radial station. Conformable rotor designs with 20 degrees of sweep at 93.5-, 90- and 80-percent radius and designs with 10, 30 and 40 degrees of sweep at 0.935R were examined. In each case the twisting moment resulting from chordwise center-of-gravity offset was made to match that of the baseline UH-60A blade by adding leading edge weight immediately inboard of the sweep

position to counterbalance the swept weight. The twisting moment imparted to a blade by a swept tip is dependent upon blade flatwise loading in the tip region. Positive lift at the tip twists the blade nose down; downloading twists the blade nose up. Uniform and nonuniform inflow results described in Reference 2 predicted negative lift at the tip of the advancing blade which tended to untwist the blade and improve rotor performance relative to an unswept blade. As described earlier, the coupling between the blade response analysis and the inflow analysis was improved to eliminate discrepancies in the treatment of blade plunging velocities. Apparently as a result of this change and the modeling of radial flow effects at the tip, advancing blade downloads are generally less than previously predicted and the noseup twisting moment produced by tip sweep is less significant. Figure 11 illustrates the airload distributions predicted with variable inflow for the baseline UH-60A rotor at the cruise condition. Download on the advancing blade tip is only slightly negative. Figure 12 compares the tip elastic twist for the baseline UH-60A blade and for various swept tip conformable rotor blades. For blades of the same stiffness, increasing sweep from 0 degrees to 20 degrees reduces the one-per-rev lateral twisting component characteristic of the straight cambered blade primarily by increasing retreating blade twist. Reducing torsional stiffness on a blade with 20 degrees of tip sweep produces a general nosedown shift in elastic twist as a result of the strong negative pitching moment of the cambered airfoil section. The nosedown twisting is least on the advancing blade where tip sweep effects tend to produce an opposing noseup moment. Relative to a straight blade, increasing tip sweep produces reduced elastic twist at ψ = 90 degrees and increased twist at $\psi = 270^{o}$. Relative to the baseline UH-60A blade, however, tip sweep in conjunction with reduced stiffness does not produce noseup advancing blade and nosedown retreating blade twisting because of the cambered airfoil. These results suggest that tip sweep would be more effective in producing positive $\theta_{E_{1s}}$ on blades with symmetrical airfoil sections or minimal camber.

Accurate prediction of advancing blade tip angle of attack and loading are critical to the evaluation of the conformable rotor concept. Not only are the aeroelastic effects of sweep dependent on tip loading, but the degree to which the performance of a given rotor can be improved by changing elastic twist depends upon the details of advancing blade conditions. At high advancing blade Mach numbers and for airfoil sections subject to severe drag divergence effects, even a slightly negative angle of attack could cause severe drag penalties and produce unwanted negative lift. The Y200 program using the nondistorted wake variable inflow model predicts that at 145 knots and design gross weight the -16-degree twist UH-60A blade advancing tip angles of attack are no more negative than -1 degree. Good agreement between total measured and calculated rotor power required (Figure 10a) suggests that predicted loading distributions are not significantly in error. Underprediction of flatwise bending moments (Figure 10b) suggests that actual tip-down advancing blade loads are larger than predicted values. Test data detailing the azimuthal airloading distribution for high twist blades such as the UH-60A blade are, unfortunately, not available and the adequacy of the current aerodynamic representation cannot easily be judged. To

further assess the validity of the analysis, airloads measured on low twist CH-53 blades and reported in Reference 9 were examined. Under the flight program described in Reference 9, a -6-degree twist CH-53A blade was instrumented with pressure transducers and airloads determined at five spanwise locations. Downloading of the advancing tip was measured at advance ratios above 0.2. It is not possible to use CH-53A results to estimate UH-60A loading because of differences in number of blades, disc loading, shaft angle and tip geometry, although it would seem likely that the -16-degree twist UH-60A blade should experience at least as much tip download as the -6-degree twist CH-53A blade. Correlation between CH-53A results and Y200 predictions using variable inflow was examined for condition 21 of Reference 9 ($\mu = 0.37$, $C_L/\sigma = 0.06$). Measured and calculated airloads at the 95-percent radial station are shown in Figure 13. The general agreement between the two distributions is good. The test results do, however, show more negative loading in the second quadrant. References 10 and 11 show that wake distortion can have significant effects on advancing blade inflow distributions, at least at low speeds. Part of the difference between calculated and measured shown in Figure 13 may result from this effect. The calculated angle of attack at $\psi = 90^{o}$ is approximately zero degrees while the measured angle is estimated to be -1.5 degrees. An angle of attack discrepancy of this amount would not be expected to give rise to large errors in tip sweep effects or calculated performance. If the analysis is equally reliable for high twist blades, predicted results should be reliable.

---

9. Beno, E., CH-53A MAIN ROTOR STABILIZER VIBRATORY AIRLOADS AND FORCES, United Technologies Corporation, Sikorsky Aircraft Division, Report SER 65593, NASC Report, Naval Air Systems Command, Washington D.C., June 1979.

10. Landgrebe, A.J., and Egolf, T.A., PREDICTION OF HELICOPTER INDUCED FLOW VELOCITIES USING THE ROTORCRAFT WAKE ANALYSIS, Proceedings of the 32nd Annual National Forum of the American Helicopter Society, May 1976.

12. Landgrebe, A.J., and Cheney, M.C., ROTOR WAKES-KEY TO PERFORMANCE PREDICTION, AGARD Conference Proceedings NO. 111 on Aerodynamics of Rotary Wings, Feb. 1973, p. 1. (Also, Proceedings of Symposium on Status of Testing and Modeling Techniques for V/STOL Aircraft, AHS Mideast Region, October 1972).

Figure 14 illustrates the calculated effects of tip sweep for a conformable rotor at the cruise condition. Rotor L/D increases with tip sweep angle, especially up to 20° sweep. These performance gains result from the relief of tip compressibility losses afforded by the sweep. Blade and control system loads and vibratory hub forces are also reduced by adding tip sweep. Minimum values are predicted to occur at a 20-deg sweep angle.

Variations in airfoil camber were examined next. Radial distributions of camber which produce the twisting prescribed with uniform inflow were sought. Pitching moment coefficients of the SC 1095 and SC 1095R8 airfoil sections were shifted by an increment assumed to be independent of angle of attack and Mach number. Airfoil lift and drag data were not changed. According to the data shown in Reference 12, this camber representation is approximately correct for deflection of trailing edge tabs. For tab deflections producing $-.02 \geq \Delta c_m \geq .02$, minimal effects on lift and drag coefficients are measured, at least for low Mach numbers. Several radial distributions of Δc_m were examined with the Y200 program. Calculated elastic twist effects were similar to those found previously. Tab deflection causing noseup pitching moment produces a one-per-rev twisting which untwists the advancing blade more than the retreating blade. Although it was possible to achieve one-per-rev twisting approximating the pattern prescribed with uniform inflow, results obtained with variable inflow did not show significant performance advantage. Figure 15 illustrates the elastic twisting produced with various sets of tab deflections. A Δc_m value of + .02 produces approximately 3 degrees of untwisting on the advancing blade. Trends of blade loads and performance presented in Figure 16 show that this twist results in only a small improvement in performance relative to the baseline UH-60A rotor. Blade bending moments are generally reduced with noseup pitching moment changes. Several combinations of tip sweep and camber were examined. Results indicated a slightly beneficial effect of noseup advancing blade twisting. Relative to the baseline UH-60A rotor, maximum L/D gains of 3 percent were predicted at the cruise condition.

In order to better understand the insensitivity of performance to lateral twisting evident at the cruise condition, the Y200 program was run for a series of prescribed elastic twist patterns. In this program mode, torsional response is locked out and a time-varying twist angle is assumed. This mode of program operation permits orderly examination of the effects of elastic twisting without requiring that blades producing the twisting be designed. The six twist patterns illustrated in Figure 17 were simulated. These include -12 degrees and -16 degrees of linear twist and $\pm$ 3 degree one-per-rev lateral perturbations on each over the outer 25 percent of the blade. Each case was trimmed to the lift,

---

12. Prouty, R.W., A STATE OF THE ART SURVEY OF TWO-DIMENSIONAL AIRFOIL DATA, Journal of the American Helicopter Society, October 1975.

propulsive force and hub moments of the baseline UH-60A blade. Uniform and variable inflow performance results are shown in Figure 18. With the uniform inflow model, rotor L/D is increased with the untwisting of the advancing blade (positive $\theta_{E_{1s}}$). -16 degrees of twist is generally superior to -12 degrees. With variable inflow, however, calculated performance is essentially unaffected by twist changes. Comparison of the azimuthal distributions of instantaneous blade torque predicted with variable inflow (Figure 19) for the set of -16-degree twist blades shows that reducing advancing blade and increasing retreating blade twist does impact torque contributions but that the total torque is not significantly changed. The increased power required on the retreating side of the disc with positive $\theta_{E_{1s}}$ results from differences in the control inputs and tip path plane orientation required to trim the conformable rotor. Twist which drives advancing blade tip airloads in the positive direction and retreating blade tip loads down causes the rotor to flap back. In order to achieve the same head moments as a conventional rotor, B_{1s} must be increased.

Increased pitch applied at the root of the blade and increased negative twist in the third and fourth quadrants tends to shift loading to inboard blade sections which are generally closer to stall. Retreating blade angle of attack is further increased by the fact that rotors with + $\theta_{E_{1s}}$ twisting tend to achieve required propulsive force with less forward tilt of the tip path plane. Reduced blade element drag on the advancing blade or increased drag on the retreating blade reduces the component of rotor drag force pointing rearward, allowing the rotor to produce the same net propulsive force with less forward inclination of the tip path plane. The flatter tip path plane allows the tip vortices shed by the rotor in the azimuth range ψ = 180 to 270 degrees to remain closer to the rotor disc as they are washed downstream. This vorticity tends to produce an upwash which drives retreating blade angles of attack toward stall.

The net impact on performance of producing one-per-rev lateral twisting depends upon the relative severity of advancing blade drag and retreating blade stall. For the Black Hawk rotor at cruise, neither side of the rotor disc suffers severe penalties; moreover, the gradients of advancing and retreating blade power with respect to twist changes are essentially the same.

In order to see if the above results held true at other flight conditions, and to possibly identify twisting patterns which matched baseline performance at cruise but provided advantages as airspeed or lift was increased, performance was calculated for the six twist patterns of Figure 17 at V = 80 kn/16,450 lb gross weight, V = 175 kn/16,450 lb and V = 145 kn/19,000 lb gross weight. At the low speed condition neither advancing nor retreating blade torque changed significantly with impressed twist changes, and the net performance effect was negligible. At the high lift condition the rotor is closer to stall on the retreating blade. As a result, increases in $\theta_{E_{1s}}$ cause retreating blade torque to increase faster than advancing blade torque decreases. The net effect

for a -12-degree twist blade is detrimental (Figure 20). For the high speed condition, increased advancing blade Mach numbers and higher retreating blade angles make performance more sensitive to twist changes. The variable inflow results shown in Figure 21 suggest that + θ_{E1s} improves the performance of a -16-degree twist blade but severely degrades the performance of a -12-degree twist blade. Comparison of blade torque signatures (Figure 22) shows increased sensitivity to twist changes. Positive θ_{E1s} on the low twist blade drives the rotor into severe stall in the fourth quadrant.

A series of impressed twist cases was also run for variations in one-per-rev cosine twisting and in two per rev twisting. Cases examined flight at 145 kn and 175 kn at design gross weight. Again, only small performance advantages were predicted to result from $\pm$ 3-degree changes in tip twist.

Based on the above, it was clear that a conformable rotor design providing large improvements in performance at practical UH-60A flight conditions was not forthcoming. A design which offered a small performance advantage at cruise was selected for evaluation of performance, rotor loads, vibration and handling qualities characteristics. The design selected includes a 4 to 1 reduction in torsional stiffness outboard of 50-percent radius, -12 degrees of nonlinear twist, a 30-degree swept tip at the 93.5-percent radius and a trailing edge up tab deflection providing + .02 Δc_m inboard of the 80-percent radius. The increased tip sweep and reduced torsional stiffness tend to drive advancing blade angles of attack to approximatley zero, which should have generally beneficial effects on forward flight performance and blade stresses. In addition, the more powerful swept tip and reduced stiffness improve hover performance by increasing static windup. The increased windup in hover and forward flight make the reduction in built-in twist from -16 to -12 degrees appropriate. The + .02 c_m shift over the inner 80 percent of the blade will tend to untwist the advancing blade, which is expected to provide at least small performance advantages. Tab deflection was not made beyond 0.8 R to avoid adverse effects on high Mach number section drag characteristics. The camber change reduces the magnitude of steady nosedown blade pitching moment, which will reduce the steady loads on the flight controls. The behavior of this conformable rotor design is compared to that of the UH-60A rotor in the following section.

UH-60A CONFORMABLE ROTOR EVALUATION

The conformable rotor design defined above was compared to the UH-60A rotor on the basis of performance, rotor loads, vibratory hub loads and effects on aircraft stability and control characteristics and maneuver capability. Performance and rotor load comparisons were made for a range of airspeeds at design gross weight (16,450 lb) and alternate gross weight (20,300 lb) at 4,000 ft pressure altitude and 95° F. The rotor was trimmed to a propulsive force consistent with a 27 ft^2 aircraft equivalent flat plate area. Level flight and autorotative descent characteristics were compared at 60 knots. The single blade fixed hub version of Y200 was used with nonuniform inflow.

PERFORMANCE AND ROTOR SYSTEM LOADS

Figures 23-25 present calculated results for the two rotors. Total rotor power required and rotor lift to equivalent drag ratios are presented in Figures 23 and 24. At design gross weight the conformable rotor achieves slight improvements in performance as a result of decreased advancing blade twist. Power savings of 30 hp are predicted at the cruise condition. This power reduction translates into a 15-lb savings in mission fuel or a 1-knot increase in speed. At the 145-knot alternate gross weight condition, increased retreating blade twist contributes to stall on the conformable rotor in the fourth quadrant. The increased twist results from the nosedown moments applied by the swept tip and, once the blade is stalled, from the nosedown pitching moment in stall. The reduced torsional stiffness increases the elastic response which results from these moments.

In order to examine effects of compressibility on conformable rotor benefits, the two rotors were compared for a range of temperature and altitude conditions which vary advancing tip Mach numbers at the advance ratio and lift coefficient of the cruise guarantee condition. Results presented in Figures 23b and 24b show that for a 10 percent increase in hover tip Mach number (T = 0° F, h_p = 7,250 ft), the conformable rotor provides a savings of 100 horsepower or an 8-percent increase in L/D.

Blade load data compared in Figure 25 show that the conformable design produces lower flatwise and edgewise blade moments up to 145 knots airspeed. At 175 knots, positive tip lift in the area over the nose excites blade torsional response at three per rev, which increases the three-per-rev components of flatwise and edgewise bending moment. Pushrod loads and four-per-rev vertical hub loads (Figures 25c and d) are lower for the conformable rotor at design gross weight but are slightly higher than those of the baseline rotor at alternate gross weight.

LOW-SPEED FLIGHT CHARACTERISTICS

Behavior of the conformable and baseline rotors was compared for a low-speed flight condition (60 knots) to determine whether any positive or

negative effects on nap-of-the-earth flight capability were projected. Autorotation at 60 knots was also simulated and results were compared. A nondistorted wake inflow was assumed in each case. Results show no effect on power required in level flight, slight (10%) increases in vibratory hub vertical shear for the conformable rotor and slight (15%) decreases in blade moments and pushrod loads. It should be pointed out that correlation between measured trends of vibration and analytic predictions has historically been poor in transition and descending flight regimes. For these flight conditions in which the wake remains close to the rotor or passes back through the rotor, exact determination of tip vortex strength and position and simulation of the aerodynamics of close blade-vortex passage or intersection are critical. Modeling of wake distortions is available within the inflow analysis. However, because Y200 employs a lifting line aerodynamic model and in the present study steady aerodynamic data, it is not well suited to prediction of the airloads resulting from close blade-vortex passage. In light of this situation, the additional effort and computational expense required to simulate the effects of wake distortion on trailing vortex position was judged to be unwarranted. At these low speed conditions the camber change and the increased tip sweep have little effect on elastic response. The difference in vibratory elastic twist between UH-60 and conformable rotors is less than 0.5 degree. Effects on performance, vibration and blade loads would not be expected to be significant.

VERTICAL RATE OF CLIMB CAPABILITY

The vertical rate of climb capability of the conformable rotor was evaluated with the Circulation Coupled Hover Analysis Program. Static twist of the conformable rotor is -12 degrees. Windup in hover increases twist to approximately -22 degrees (compared to -17 degrees for the UH- rotor). Relative to the UH-60A rotor, this increase in twist provides a savings of approximately 30 horsepower for a 480-ft/min VROC or an increase from 480 to 660 ft/minute in the climb rate possible using 95 percent of installed intermediate power.

HANDLING QUALITIES CHARACTERISTICS

The effects of the reduced torsional stiffness and increased tip sweep of the conformable rotor on UH-60A stability and control characteristics were analyzed using the Sikorsky flight dynamics model, GENHEL, and the Y200 program. GENHEL is Sikorsky's standard method for predicting aircraft handling qualities characteristics. The analysis performs a timewise integration of the rotor and aircraft equations of motion and determines six-degree-of-freedom response for steady state and maneuvering flight. The rotor model includes rigid blade flapping only. Rotor aerodynamics are based on two-dimensional strip theory. Examples of the correlation between flight test data and GENHEL predictions are shown in Figure 26. UH-60A transient response to a longitudinal pulse is simulated quite accurately with the GENHEL model.

Because GENHEL does not treat blade aeroelastic response, the approach adopted in analyzing the conformable rotor was to define aircraft trim

conditions with GENHEL and input the resulting rotor force and moment requirements, together with the shaft orientation, into Y200. This procedure established the control inputs and the tip path plane orientation required for the conformable rotor to trim the basic UH-60A airframe. At these trim conditions rotor derivatives were obtained from Y200 by perturbing the control inputs θ_{75}, A_{1s} and B_{1s}, the velocities v_x and v_z and aircraft pitch rate q. Pitch rate derivatives, which are not normally available from Y200, were obtained by exercising the multiblade transient response option of the program for specified rates of hub pitching. Aircraft stability and control derivatives were calculated in this fashion for the conformable rotor and the Black Hawk rotor at 60, 120 and 150 knots at design gross weight and sea level standard conditions. Control derivatives of the rotors were compared directly. Rotor stability derivatives were combined with the derivatives obtained for the rest of the aircraft from the flight dynamics model and aircraft roots calculated. This approach put changes in rotor stability derivatives in perspective with respect to contributions of other aircraft components.

The control inputs required of the two rotors for trim are illustrated in Figure 27. As shown, slightly higher collective and longitudinal cyclic pitch inputs are required for the conformable design. These trends are consistent with the increased steady nosedown elastic twist and noseup twisting on the advancing blade. The most significant effects noted with regard to the control derivatives are presented in Figure 28. The two collective derivatives $Z_{\theta 75}$ and $M_{\theta 75}$ indicate reduced sensitivity. The former indicates a requirement for 20% more collective range, although this is not entirely consistent with the trim data which showed only a 1-degree increase (7%). This results from cyclic and velocity interactions on trim. The reduced pitching moment with collective is beneficial in that it reduces the control coupling. Only small changes in the longitudinal derivative, $M_{B_{1s}}$, were experienced throughout the speed range evaluated, as indicated in Figure 28. The only significant effect evident in comparing the stability derivatives is a reduction in Z_{v_z} for the conformable rotor. This will result in reduced gust sensitivity.

The effects of the conformable rotor on overall aircraft stability were determined by calculating the eigenvalues of the linearized equations of motion. The rotor longitudinal stability derivatives obtained from Y200 were substituted for the corresponding derivatives obtained from GENHEL. Rotor lateral derivatives were not changed. The effects of changes in longitudinal stability derivatives on aircraft stability are summarized in the root locus plot presented in Figure 29. Some small degradation in the stability of the longitudinal oscillation is evident, but overall, the conformable rotor has very little impact on the stability of the aircraft. It is anticipated that the changes in stability could be accommodated within the existing UH-60A flight control system.

It is concluded from this brief evaluation that except for the reduced collective sensitivity, the conformable rotor configuration examined would have little impact on the UH-60A from a handling qualities point of view.

MANEUVER CHARACTERISTICS

An attempt was made to compare maneuver capability of the two rotors by simulating a steady coordinated 60-degree angle of bank turn at 160 knots airspeed at 4000 ft h_p and 95° F. The rotor-alone steady state mode of Y200 was used to simulate the steady state portion of the turn. Rotor response was calculated for a series of increasing values of load factor starting at 1.0g. Uniform inflow was initially assumed. Each rotor stalled before developing the target 2.0 g of thrust. The UH-60A rotor stalled at approximately 1.4 g and the conformable rotor at 1.3 g. The discrepancy between these load factors and higher values demonstrated in flight is not well understood. Part of the difference may result from the use of a steady aerodynamic model and uniform inflow. Unsteady aerodynamic effects are known to provide increased lifting capability (Reference 13). Selected cases were repeated with nonuniform inflow, with only slight increases in load factor predicted. The earlier stall of the conformable rotor appears to result from the same effects described earlier in the discussion of the impressed twist cases. Increased B_{1s} promotes stall inboard on the blade in the fourth quadrant.

It appears from these turn calculations, the 145-knot alternate gross weight level flight results and the impressed twist cases run at high gross weight that the maneuver capability of a conformable rotor producing the lateral twisting studied herein would be less than that of a conventional rotor. Because results near stall are influenced by unsteady aerodynamic effects, the present results obtained with a steady aerodynamic model should be reviewed when results on conformable rotor model tests become available.

---

13. Bellinger, E.D., ANALYTIC INVESTIGATION OF THE EFFECTS OF BLADE FLEXIBILITY, UNSTEADY AERODYNAMICS, AND VARIABLE INFLOW ON HELICOPTER ROTOR STALL CHARACTERISTICS, NASA CR-1769, September 1971.

UH-60A CONFORMABLE ROTOR RISK ASSESSMENT

The design evaluation task indicated that there was a potential for improving rotor performance through control of blade twisting. The combination of design variables used on the current baseline UH-60A achieves performance very close to the optimum, and the latitude for improving performance by altering dynamic twist is calculated to be small. Determining whether this conclusion is generally true for current rotors was beyond the scope of this effort. Controllable Twist Rotor Wind Tunnel data (Reference 14) show a mild effect of one-per-rev twist changes on performance. A one-per-rev twisting which provides optimum performance is identified at each flight condition. The desired twisting varies with advance ratio, lift coefficient and steady twist. For the flight conditions tested under that program, achieving one-per-rev cosine and sine components of twist within 3 degrees of the ideal values produced torque coefficients within 4 percent of the minimum value. The conclusion regarding the potential for improving performance by changing dynamic twist may be that dynamic twist changes have a large effect on performance only for rotor designs and flight conditions exhibiting severe local stall or compressibility losses. Reduced torsional stiffness and increased tip sweep do provide the opportunity for increasing effective twist in hover without increasing built-in twist and forward flight stresses.

The design evaluation further showed that for blades involving stiffness reductions on the order four to one over the outer half of the blade and fairly substantial amounts of tip sweep and tab deflection, rotor system loads, vibratory hub forces and handling qualities characteristics were not significantly different from those of the UH-60 rotor. This conclusion is significant in itself because it suggests that blade materials or designs which might be attractive for other reasons but which reduce torsional stiffness can be considered without undue concern for torsional response effects, but only if significant tip sweep is provided. At high lift conditions the reduced torsional stiffness and increased tip sweep produced high retreating blade twist which contributed to aggravated inboard stall. As a result of this effect, a conformable rotor of the type designed may be subject to poorer performance for those conditions where retreating blade stall is more of a factor than advancing blade compressibility losses. Manufacturing requirements and nuisance vibration resulting from blade-to-blade dissimilarities are two other risk areas for reduced stiffness blades. These are discussed below.

MANUFACTURING REQUIREMENTS

The structural design study described earlier used hypothetical blade stiffness and mass properties without regard for blade materials or

---

14. Lemnios, A.Z., and Howes, H.E., WIND TUNNEL INVESTIGATION OF THE CONTROLLABLE TWIST ROTOR PERFORMANCE AND DYNAMIC BEHAVIOR, USAAMRDL TR-77-10, Eustis Directorate, US Army Air Mobility R&D Laboratory, Fort Eustis, VA, June 1977, AD 042481.

fabrication approaches. A brief study was conducted to identify materials and design approaches which provide the required reduction in torsional stiffness without experiencing high levels of torsional or bending strain. The blade twist rates, torsional moments and bending moments calculated during the design evaluation were used in evaluating the feasibility of various design approaches. Based on these applied loads, several alternatives were selected which either individually or combined can accomplish the goal of reduced outboard torsional stiffness without significantly affecting manufacturing complexity, blade weight or cost. The approaches are described below:

a) Composite Structure

The use of composites for the primary blade structural material provides a high degree of design flexibility. Varying the fiber angle from a $\pm$ 45° orientation to 0° to the span direction will reduce torsional moduli by a factor of 2 to 3, depending on the fiber material. Of the available composite materials, fiberglass is the preferred type because of its low stiffness and high strength characteristics. If an outboard spar geometrically identical to the titanium spar (except for wall thickness) was made primarily of unidirectional (0°) s-glass, the bending stiffness and weight of the UH-60A blade could be matched with approximately 1/3 to 1/4 the torsional stiffness.

b) Structural Modifications

The d-spar structure used on the titanium UH-60A blade results in a high torsional stiffness to weight ratio, which was a design requirement. The use of a c-spar structure using the structural materials will provide approximately a 45-percent reduction in torsional stiffness with little change in the weight and flapwise stiffness. It is precisely for this reason that c-spar structure without a structural web is usually disregarded when high GJ/weight is a design goal.

c) Airfoil Thickness Modifications

Reducing the airfoil thickness ratio over the outboard part of the blade will provide reduced torsional stiffness with accompanying similar percentage reductions in the flapwise bending stiffness. For the same structural material and weight, the GJ and flatwise EI are approximately proportional to the square of the airfoil thickness ratio for typical rotor blade structure. The type of reductions in GJ desired (75%) for the conformable rotor cannot be practically met with this design alternative alone; however, in combination with the other approaches, the goal can easily be achieved.

d) Effective torsional stiffness modifications can also be achieved by utilizing the potential stiffening/softening provided by aerodynamic forces. By tailoring the elastic axis and center-of-gravity axis distributions, localized effective stiffness changes can be realized with little structural complication. However, a thorough understanding of the stability characteristics of such an aeroelastic configuration is necessary before serious consideration is given to this approach.

Inboard spar structure would be different from that of the outboard areas in order to increase the inboard GJ to the desired values. This could be accomplished using the same design alternatives that were used to achieve reduced stiffness:

a) The addition of $\pm 45^{o}$ plies in a composite structure, either of graphite (for maximum weight penalty) or fiberglass.

b) Transition of an outboard c-spar into a d-spar structure.

c) Increases in airfoil thickness ratio, which also increases flatwise stiffness.

EFFECT OF BLADE DISSIMILARITY ON VIBRATION

Reduction in torsional stiffness can be expected to increase the amplitude of the elastic twist which results from a given applied moment. Blades of reduced torsional stiffness will, therefore, tend to experience larger differences in elastic twist and angle of attack for fixed amounts of blade dissimilarity. The forces and moments transmitted to the fixed system as a result of blade dissimilarities may therefore be larger and aircraft vibration at one, two, three per rev, etc, aggravated. This type of vibration must be minimized at the source because it would be impossible to provide vibration reduction devices which would be effective over such a wide range of frequencies and for arbitrary levels of input at the various frequencies. If a conformable rotor aggravates this vibration effect, it would be a serious drawback.

In order to provide a first indication of the magnitude of this effect, the vibratory hub forces resulting from a given set of hypothetical blade dissimilarities were examined with the Y200 program for the UH-60A and conformable rotors. The assumed differences included those which might result from manufacturing deviations and those which might result from field damage. The method used to analyze this problem was first to determine the set of harmonic forces and moments applied to the hub by three undamaged blades using the Y200 program with variable inflow. Then, maintaining the same control angles and inflow distribution, the response of a single damaged blade and the forces fed to the hub were calculated. Ideally the rotor inflow distribution should have been changed to reflect the wake produced by the three normal blades and the one odd blade. In the absence of such an analytic capability the present approach was adopted and is assumed to be adequate. Effects of hub response on blade motions and applied loads were not modeled. Total hub

forces and moments were then obtained by filtering the inputs of one damaged and three undamaged blades into the fixed system.

Previous analytic studies of blade ballistic damage effects have shown that of the many types of dissimilarity which may be present in a set of blades, aerodynamic pitching moment and chordwise center-of-gravity differences have the most significant effects on torsional response. Deviations in these parameters which result from manufacturing are compensated for in preparing blades for flight. Blades are whirled on a test stand and pitching moment versus collective pitch characteristics compared to a master blade. Tabs are then deflected to compensate for errors in absolute pitching moment, and tip weights are moved in the chordwise direction to compensate for discrepancies in pitching moment versus collective pitch slope. If there are significant differences in the radial distributions of camber or c.g. offset, the corrections made at zero forward speed may not be satisfactory for eliminating non n/rev vibration problems at forward speed.

In order to determine the significance of this effect for a conformable rotor, cruise vibratory hub loads were determined for a series of blades assumed to have camber and c.g. deviations ranging from zero to the maximum which can be overcome with the tip weight and tab deflection provisions of the UH-60A blade. Positive and negative extremes were examined. Camber and center-of-gravity deviations were assumed to exist over various spanwise extents, and the tab deflection or tip center-of-gravity correction required to match design hover pitching moment characteristics was included. In general the residual non n/rev fixed system forces and moments calculated for the conformable rotor were approximately half of the corresponding UH-60A rotor forces. Figure 30 illustrates the harmonic components of axial force for UH-60A and conformable rotors for representative cases. One-per-rev loads are clearly the most significant. Although the changes in steady and one-per-rev torsional response were generally greater for the conformable rotor than for the UH-60A rotor, for the eight cases considered the changes in one-per-rev hub forces were calculated to be less. The reason for this effect is not clear. Tracing the effects of compensating inboard and outboard camber changes on elastic response and the effect of the elastic twist on blade response and hub loads is extremely difficult. Results suggest that the conformable rotor may benefit from cancellation of the fixed system one-per-rev forces resulting from the steady and the one-per-rev changes in elastic pitch.

The second set of blade dissimilarities considered were uncompensated changes in camber or chordwise center-of-gravity position which might result from field damage, ballistic damage or icing. Y200 cases were run for changes in camber and center-of-gravity extending over the outer 7 percent of the blade. Tab deflection and tip weight position were not changed. A series of increasingly severe damages were assumed. One-per-rev hub loads were by far the most significant. For damages producing changes in effective camber, it was expected that the conformable rotor would produce larger differences in track and higher fixed system vibration

than the UH-60A rotor. Apparently as a result of increased control system stiffness assumed for the conformable rotor system and the increased tip sweep, net fixed system one-per-rev forces for the conformable rotor were, however, comparable to those of the baseline. Figure 31 compares conformable and UH-60A rotor fixed system forces for changes in tip camber. Conformable rotor axial loads are essentially the same as those of the baseline. Lateral loads are less. In order to understand these results, vibratory loads were calculated with conformable rotor tip sweep reduced from 30 to 20 degrees and then additionally with the control system stiffness reduced to that of the UH-60A rotor. Axial force results suggest that increased control system stiffness and tip sweep maintain the axial loads of the torsionally soft blade at conventional levels.

Vibratory loads resulting from localized changes in center-of-gravity position were also examined for the two rotors. Forward and aft shifts of the center of gravity which might result from damage to the outer 10 percent of the blade were simulated. Here again, loads of the UH-60A and conformable rotors were comparable. For damage producing an extreme aft shift in center of gravity, each rotor is subject to a coupled flatwise-torsion instability. The onset of this oscillation occurred on each rotor when the cg of the outer 10 percent of the blade was shifted aft by 12 percent of chord.

In summary, the results of this limited evaluation predict that the conformable rotor described above would provide little or no increase in the fixed system vibration resulting from manufacturing dissimilarities. In the case of blade to blade differences for which no compensation is provided (e.g., differences resulting from field damage), reducing blade torsional stiffness does not aggravate vibration effects if proper tip sweep and control system stiffness are provided. For the same root stiffness and sweep as the UH-60A blade, however, a four-to-one reduction in outboard torsional stiffness increased one-per-rev axial loads by 40 percent. Lateral and longitudinal loads produced by conformable and baseline designs were comparable regardless of the root stiffness. Conclusions are based on cruise results and should probably be checked at other flight conditions.

CONCLUSIONS

1. The performance of a conformable rotor employing passive in-flight variable twist control is sensitive to the detailed modeling of the aerodynamics of the advancing tip.

2. An analysis employing lifting line, steady-state aerodynamics and a variable inflow model based on a nondistorted wake geometry projects that small improvements in the performance of the UH-60A aircraft at its design operating conditions can be produced using a conformable rotor. The projected improvements tend to be within the accuracy of the analysis and are not inconsistent with the previous optimization of the UH-60A rotor design.

3. The analysis projects the following incremental improvements in UH-60A design point characteristics:

   1.2% improvement in hover figure of merit
   210-ft/min increase in vertical rate of climb
   2% increase in L/D at cruise
   1-knot increase in cruise speed
   15-lb reduction in mission fuel
   15% reduction in blade vibratory edgewise bending moments
   20% reduction in vibratory pushrod load
   no significant change in vibratory flatwise moments or 4-per-rev vibratory hub loads

4. The analysis projects that the conformable rotor will tend to degrade performance slightly at conditions where retreating blade stall is of more importance than advancing blade compressibility effects (e.g., at alternate gross weight or in manuevers). Conversely, additional improvements are possible at conditions where advancing blade effects are more critical (e.g., low altitude, low temperature, high speed).

5. Mission fuel savings produced by the conformable rotor would be significantly larger for missions involving a greater percentage of hover operation.

6. The conformable rotor produced an increase in hover figure of merit through increased twist without the usual attendant increase in forward flight vibratory flatwise bending moments.

7. Analysis shows that the conformable rotor would have little impact on the handling qualities of the UH-60A. A 7% increase in collective range would be required. A small reduction in control coupling and gust sensitivity is projected.

8. Analysis indicates no increase in the sensitivity of the conformable rotor to blade tolerances or blade damage, provided tip sweep and control system stiffness are properly selected.

RECOMMENDATIONS

1. Model tests should be conducted to verify the trends of conformable rotor performance, blade loads and vibratory hub forces predicted by the aeroelastic and inflow analyses. The predicted effects of tip sweep and camber on blade elastic response and the direct effects of the response on rotor attributes should be determined.

2. The potential for reducing vibratory hub forces by dedicating conformable rotor twisting to the reduction of n-1, n and n+1 per rev airloads should be examined.

3. The effect of wake distortions on calculated angle of attack distributions should be examined.

4. The impact of unsteady aerodynamic effects on conformable rotor performance should be assessed.

REFERENCES

1. Blackwell, R.H., and Commerford, G.L., INVESITGATION OF THE EFFECTS OF BLADE STRUCTURAL DESIGN PARAMETERS ON HELICOPTER STALL BOUNDARIES, Sikorsky Aircraft Division, United Technologies Corporation; USAAMRDL Technical Report 74-25, Eustis Directorate, U.S. Army Air Mobility Research and Development Laboratory, Fort Eustis, VA, May 1974, AD 784594.

2. Blackwell, R.H., INVESTIGATION OF THE COMPLIANT ROTOR CONCEPT, Sikorsky Aircraft Division, United Technologies Corporation, USAAMRDL TR 77-7, Eustis Directorate, USAAMRDL, Fort Eustis, Virginia, June 1977, AD A042338.

3. Blackwell, R.H., and Merkley, D.J., THE AEROELASTICALLY CONFORMABLE ROTOR CONCEPT, American Helicopter Society, 34th Annual National Forum, May 1978.

4. Kefford, N.F.K., and Campbell, B., SIKORSKY HELICOPTER DESIGN MODEL USER'S GUIDE, Sikorsky Engineering Report SER-50851, November 1973.

5. Arcidiacono, P.J., PREDICTION OF ROTOR INSTABILITY AT HIGH FORWARD SPEEDS, VOL. I, STEADY FLIGHT DIFFERENTIAL EQUATIONS OF MOTION FOR A FLEXIBLE HELICOPTER BLADE WITH CHORDWISE MASS UNBALANCE, Sikorsky Aircraft Division, United Technologies Corporation; USAAVLABS 68-18A, *U.S. Army Aviation Materiel Laboratories*, Fort Eustis, Virginia, February 1969, AD 685860.

6. Langdrebe, A.J., et al., AERODYNAMIC TECHNOLOGY FOR ADVANCED ROTORCRAFT, American Helicopter Society, Symposium on Rotor Technology, August 1976.

7. Harris, F.D., PRELIMINARY STUDY OF RADIAL FLOW EFFECTS ON ROTOR BLADES, Journal of the American Helicopter Society, July 1966.

8. Ericson, W. et al., FLIGHT LOADS SURVEY TEST REPORT, Sikorsky Engineering Report SER-70406, May 1976.

9. Beno, E., CH-53A MAIN ROTOR STABILIZER VIBRATORY AIRLOADS AND FORCES, United Technologies Corporation, Sikorsky Aircraft Division, Report SER 65593, NASC Report, Naval Air Systems Command, Washington D.C., June 1970.

10. Landgrebe, A.J., and Egolf, T.A., PREDICTION OF HELCOPTER INDUCED FLOW VELOCITIES USING THE ROTORCRAFT WAKE ANALYSIS, Proceedings of the 32nd Annual National Forum of the American Helicopter Society, May 1976.

11. Landgrebe, A.J., and Cheney, M.C., ROTOR WAKES-KEY TO PERFORMANCE PREDICTION, AGARD Conference Proceedings No. 111 on Aerodynamics of Rotary Wings, Feb. 1973, p. 1. (Also, Proceedings of Symposium on Status of Testing and Modeling Techniques for V/STOL Aircraft, AHS Mideast Region, Oct. 1972).

12. Prouty, R.W., A STATE OF THE ART SURVEY OF TWO-DIMENSIONAL AIRFOIL DATA, Journal of the American Helicopter Society, October 1975.

13. Bellinger, E.D., ANALYTIC INVESTIGATION OF THE EFFECTS OF BLADE FLEXIBILITY, UNSTEADY AERODYNAMICS, AND VARIABLE INFLOW ON HELICOPTER ROTOR STALL CHARACTERISTICS, NASA CR-1769, September 1971.

14. Lemnios, A.S., and Howes, H.E., WIND TUNNEL INVESTIGATION OF THE CONTROLLABLE TWIST ROTOR PERFORMANCE AND DYNAMIC BEHAVIOR, USAAMRDL TR-77-10, Eustis Directorate, US Army Air Mobility R&D Laboratory, Fort Eustis, VA., June 1977, AD 042481.

TABLE 1. UH-60A BLADE DESIGN PARAMETERS

Number of blades	4
Rotor type	articulated
Radius	26.833 ft
Solidity	.083
Tip speed	725 ft/sec
Offset ratio	.047
Airfoils	SC1095 and SC 1095R8
Twist	-16 deg (nonlinear)
Tip geometry	20 deg sweep at 0.935R
Lock number at SLS	8.51
Calculated frequency ratios, flatwise	2.85, 5.11, 8.02
Edgewise	4.80, 12,35
Torsional	4.22, 13.76

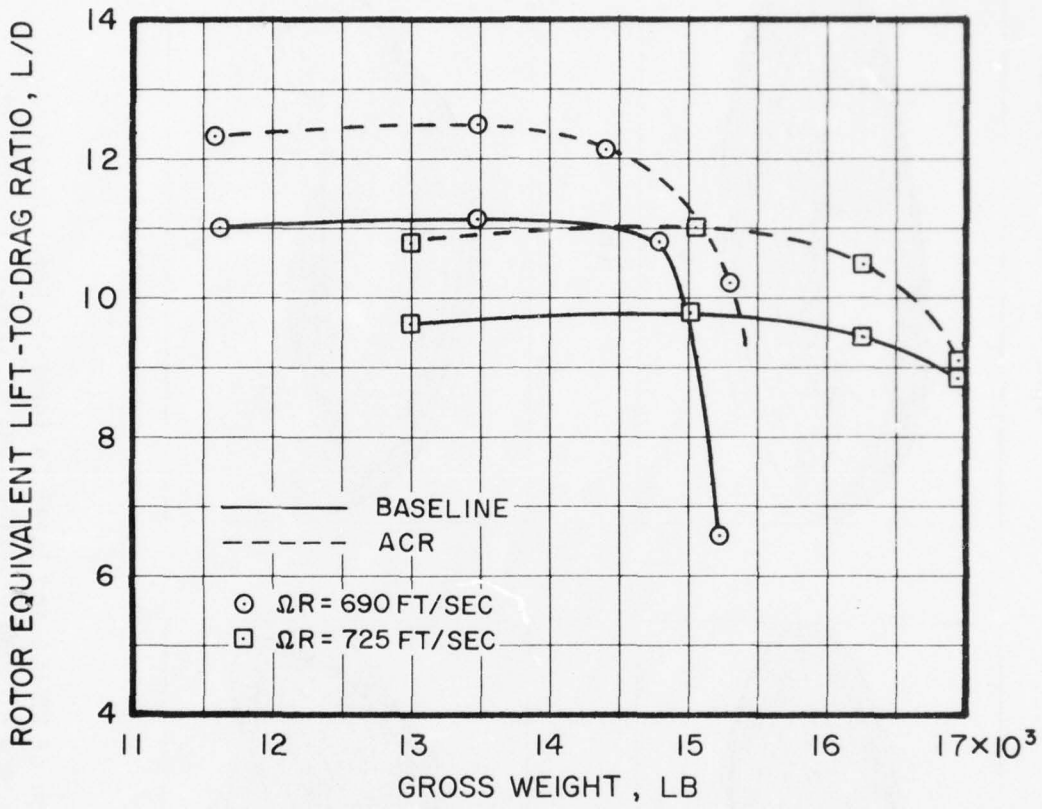

Figure 1. Improvements in Cruise L/D Predicted for an Ideal Conformable Rotor with Uniform Inflow; V = 145 kn, h_p = 4000 ft, T = 95° F.

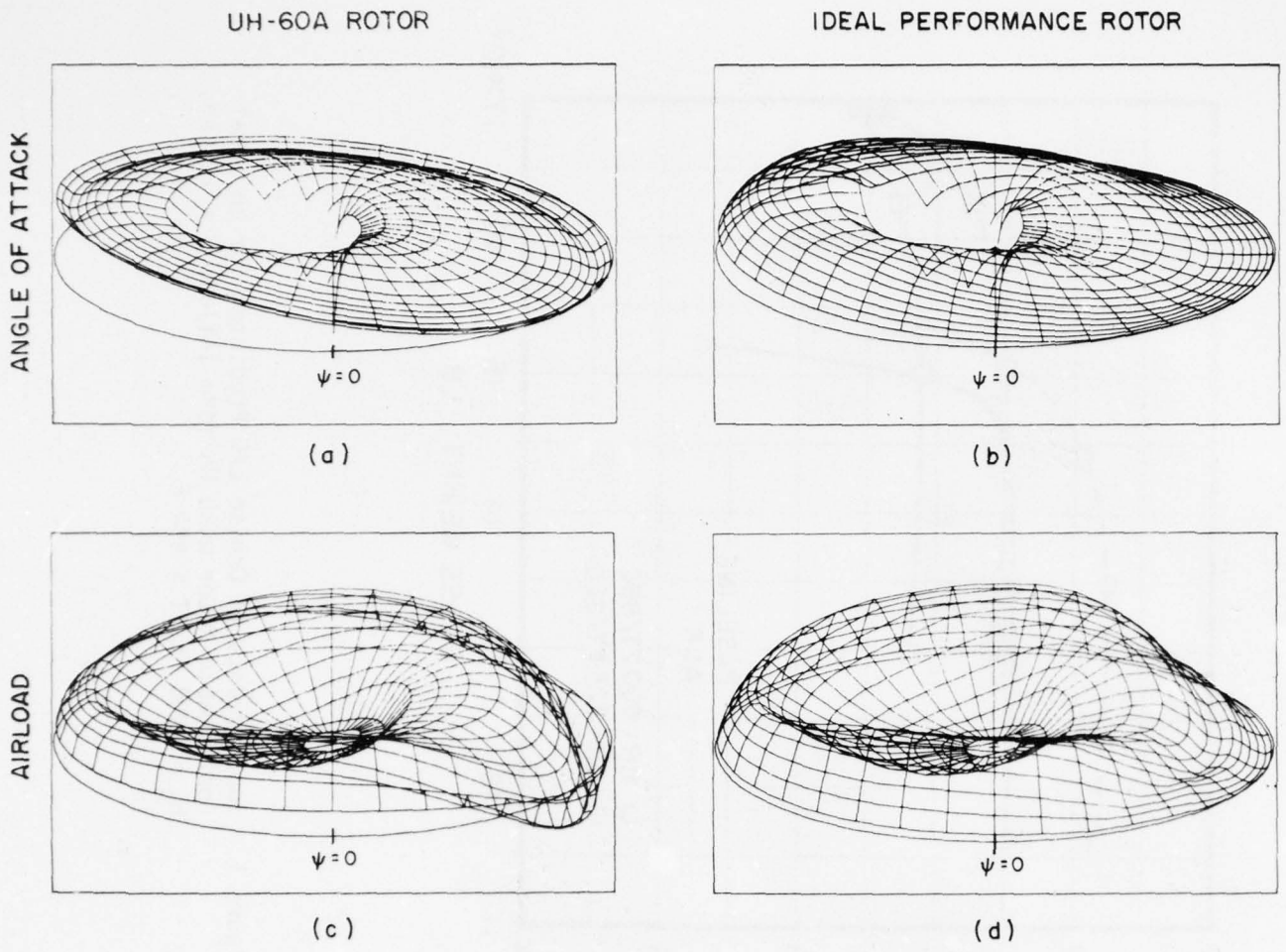

Figure 2. Comparison of UH-60A and Ideal Conformable Rotor Angle of Attack and Airload Distributions at Cruise; V = 145 kn, Gross Weight = 16,450 lb.

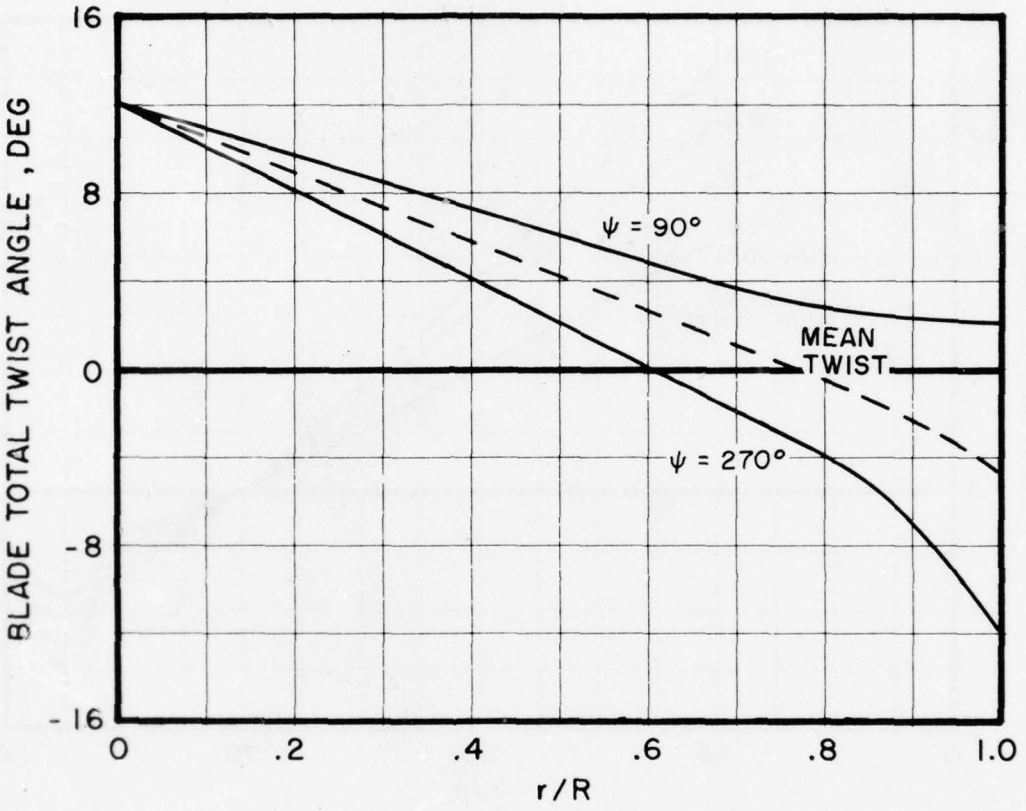

Figure 3. Twist Angle Required to Achieve Optimal Performance at Cruise; V = 145 kn, Gross Weight = 16,450 lb.

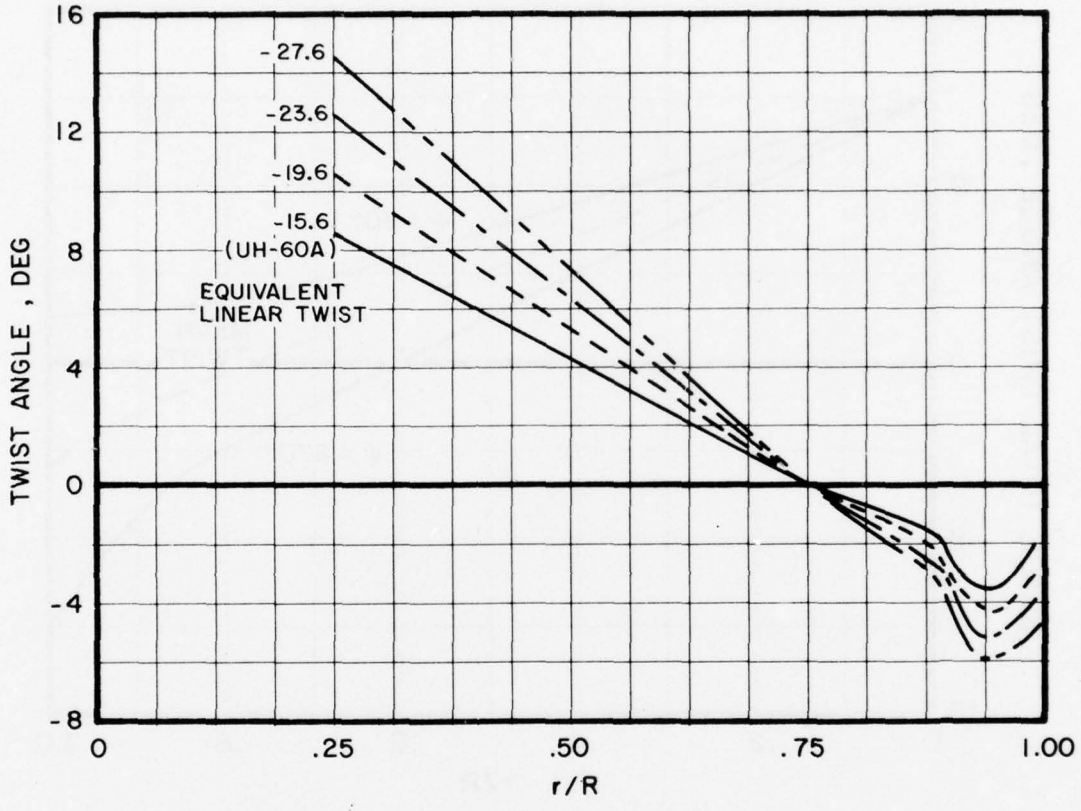

Figure 4. Nonlinear Twist Distributions Examined in Hover.

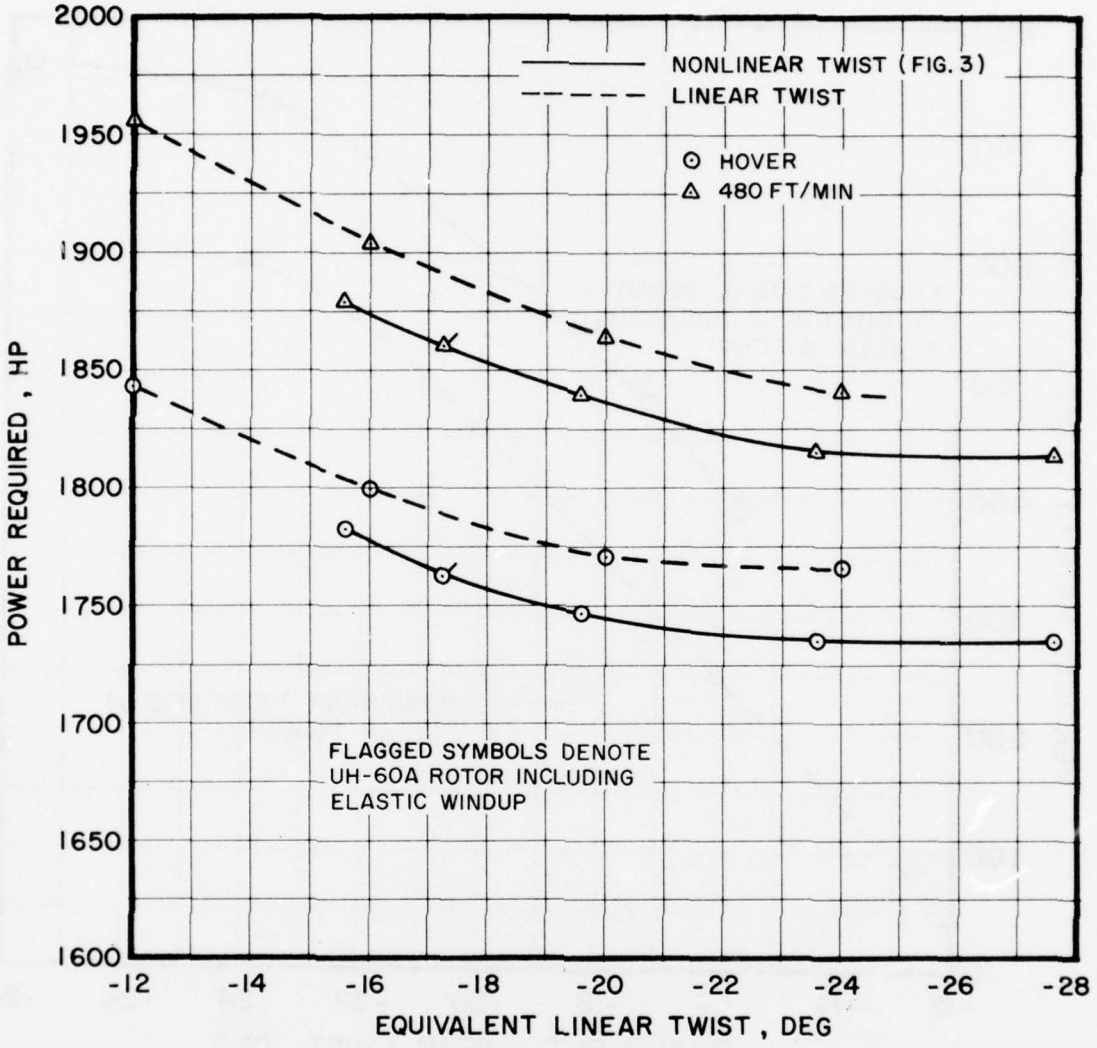

Figure 5. Variation of Hover and Climb Power Required With Twist Angle; Rotor Thrust = 16,450 lb, h_p = 4000 ft, T = 95° F.

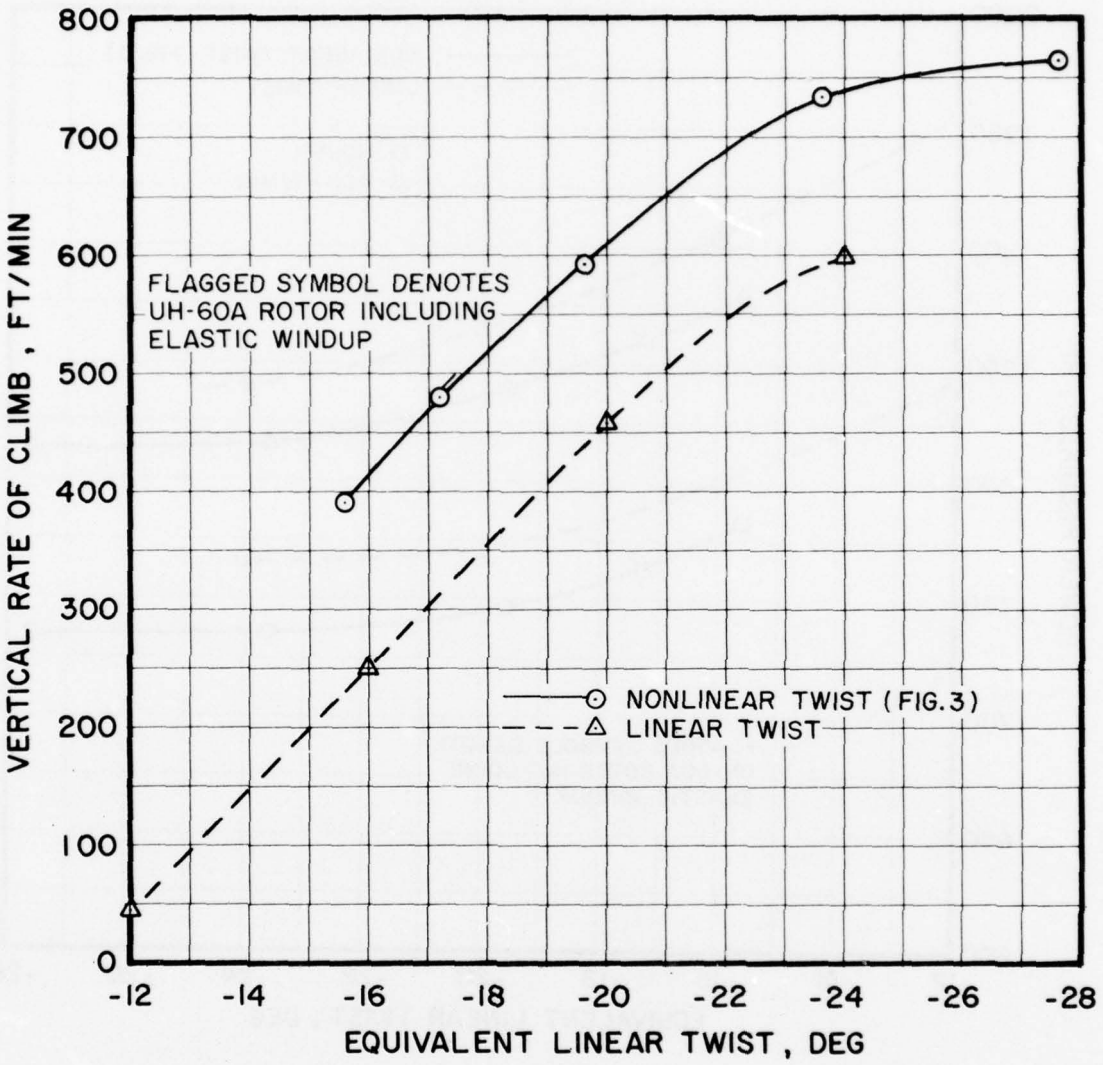

Figure 6. Variation of Rate of Climb With Equivalent Linear Twist; Rotor Thrust = 16,450 lb, h_p = 4000 ft, T = 95° F.

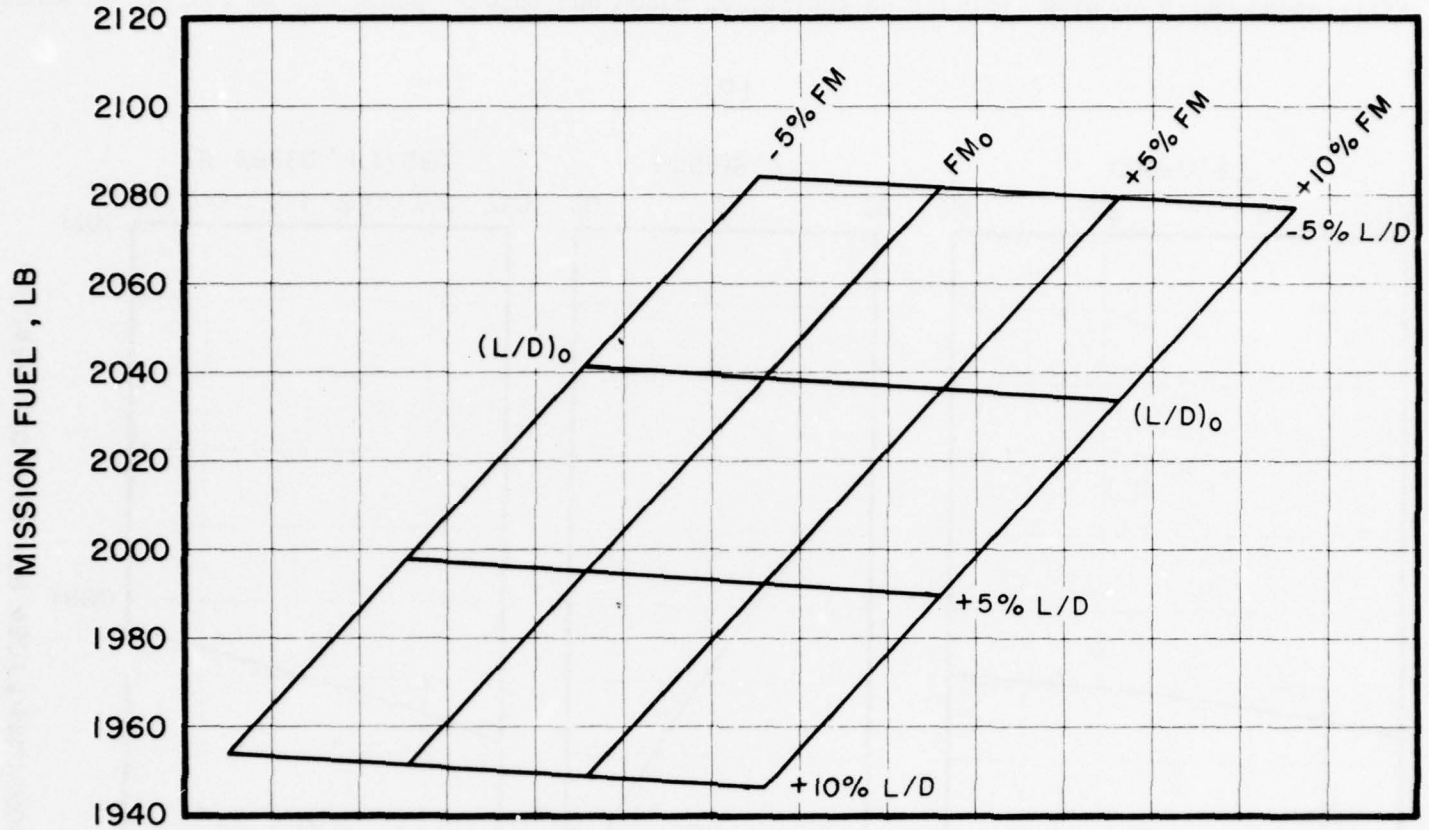

Figure 7. Sensitivity of UH-60A Mission Fuel to Rotor Figure of Merit and Cruise L/D Changes.

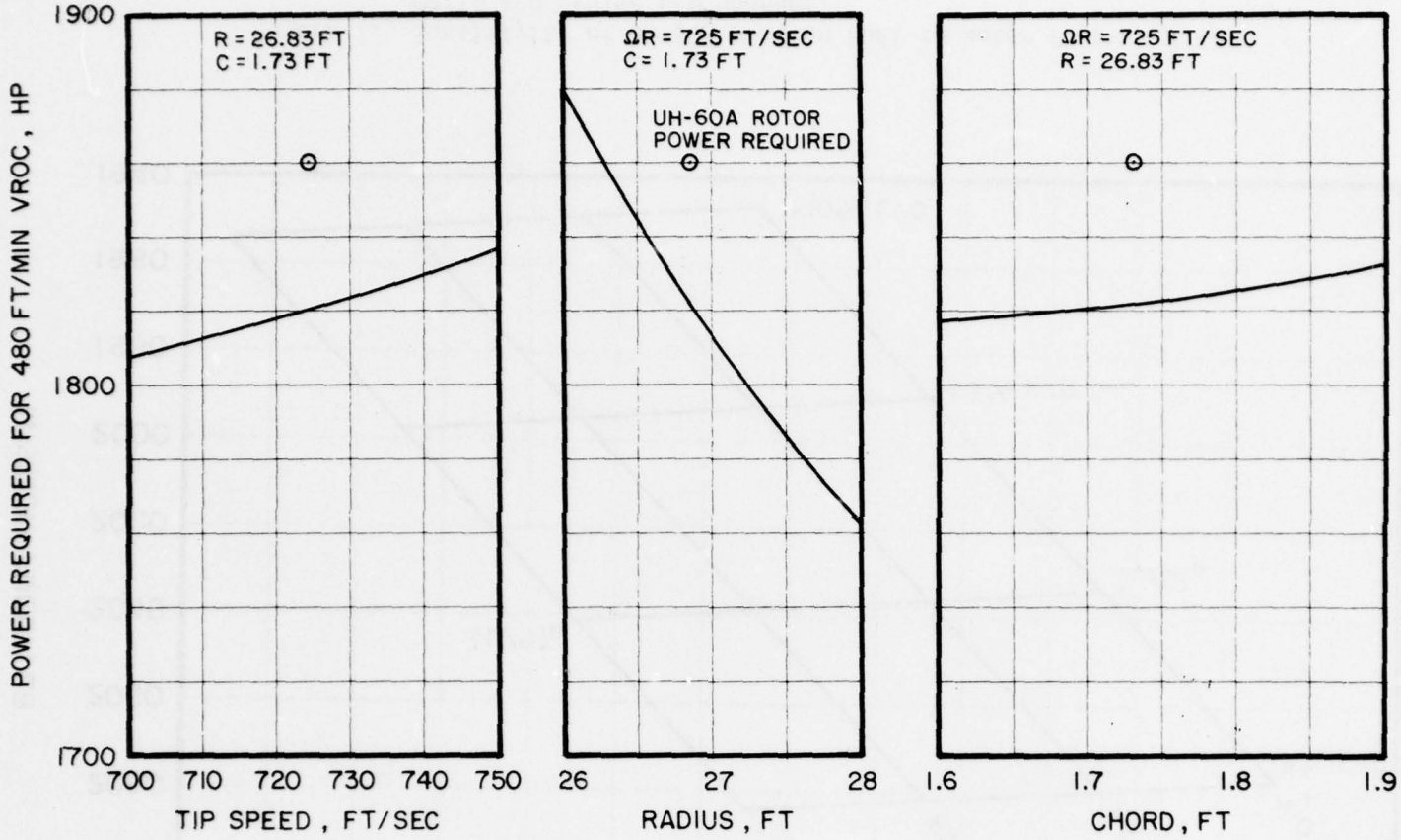

(a)

Figure 8. Effect of Tip Speed, Radius and Chord Variations on Vertical Rate of Climb Capability; Gross Weight = 16,450 lb, h_p = 4000 ft, T = 95° F, Nonlinear Twist = -24 deg.

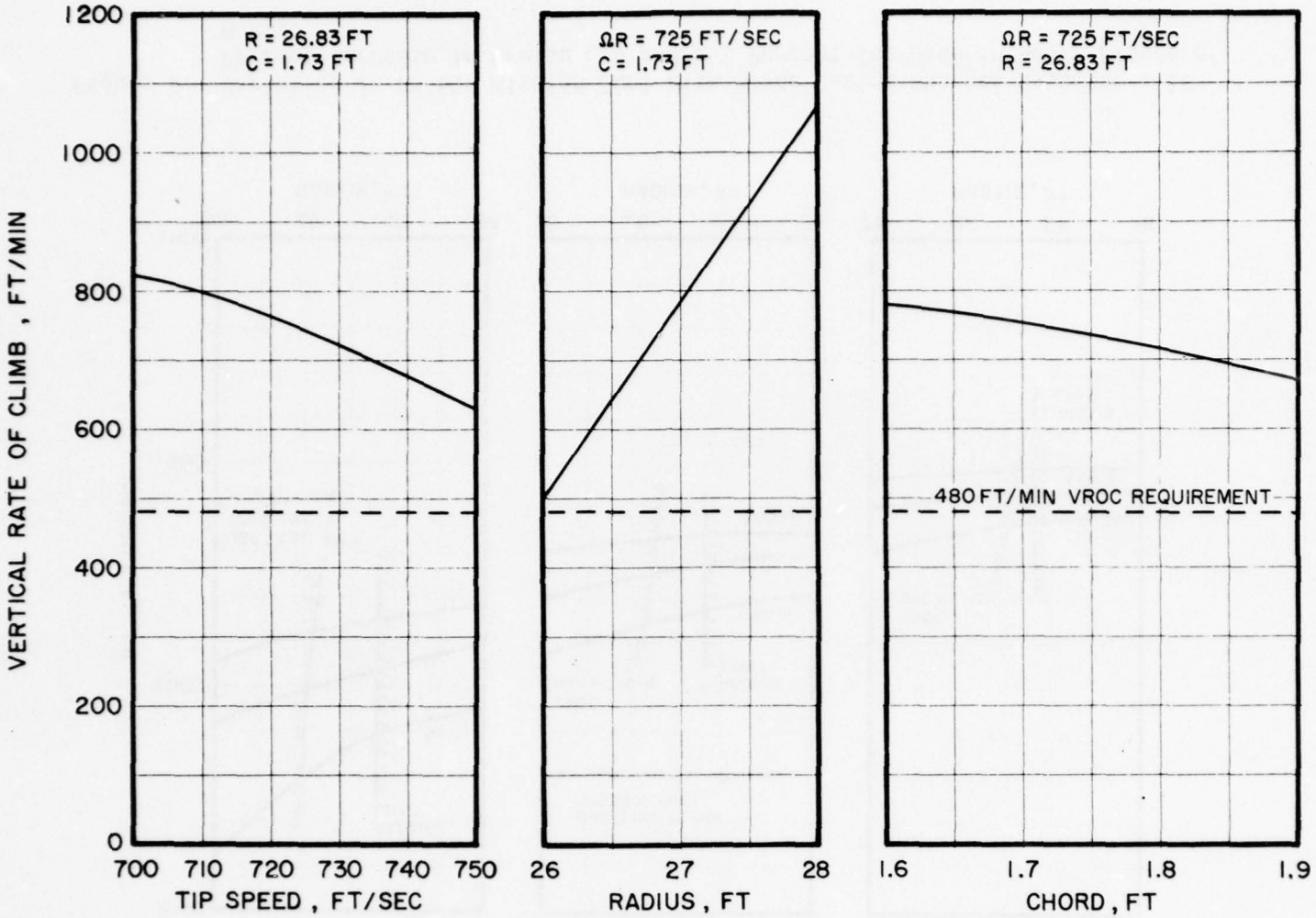

(b)

Figure 8. Concluded.

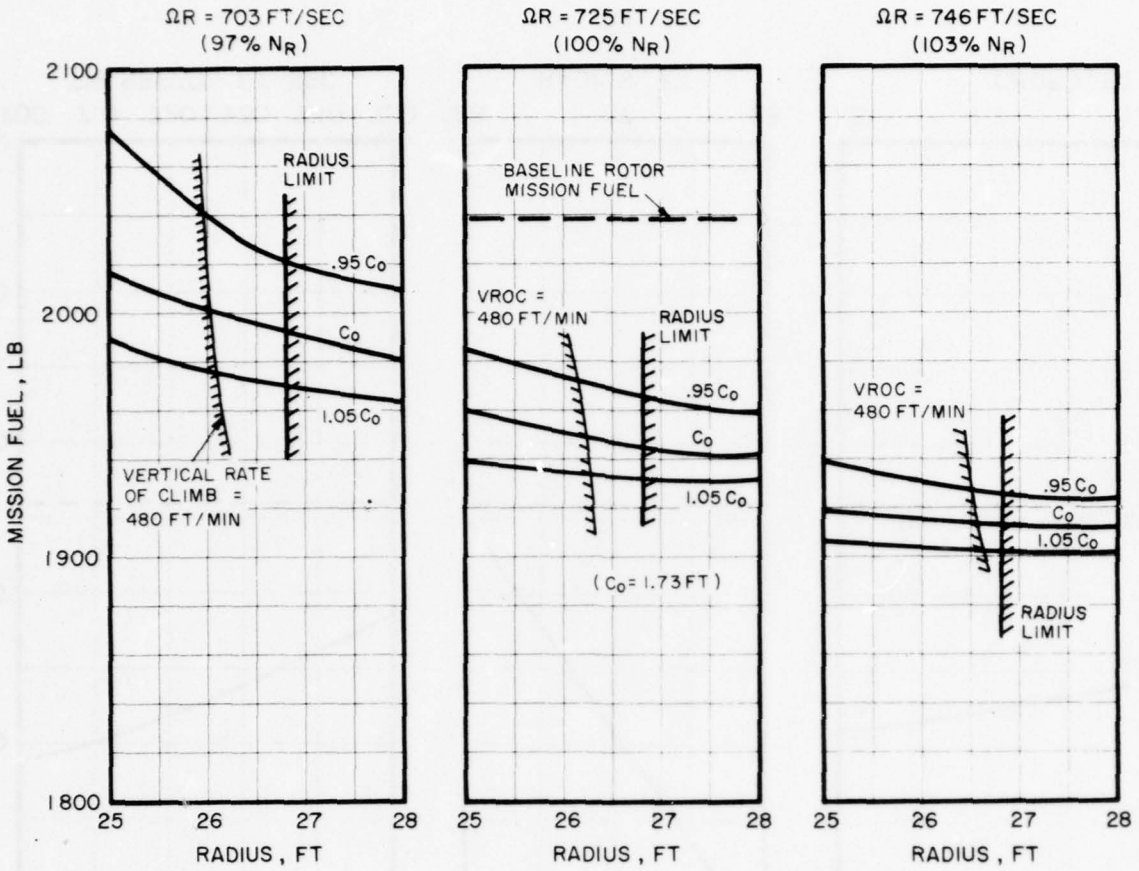

Figure 9. Variation in UH-60A Mission Fuel With Blade Design Changes Assuming a 10 Percent Increase in Cruise L/D and a 2 Percent Increase in Hover Figure of Merit.

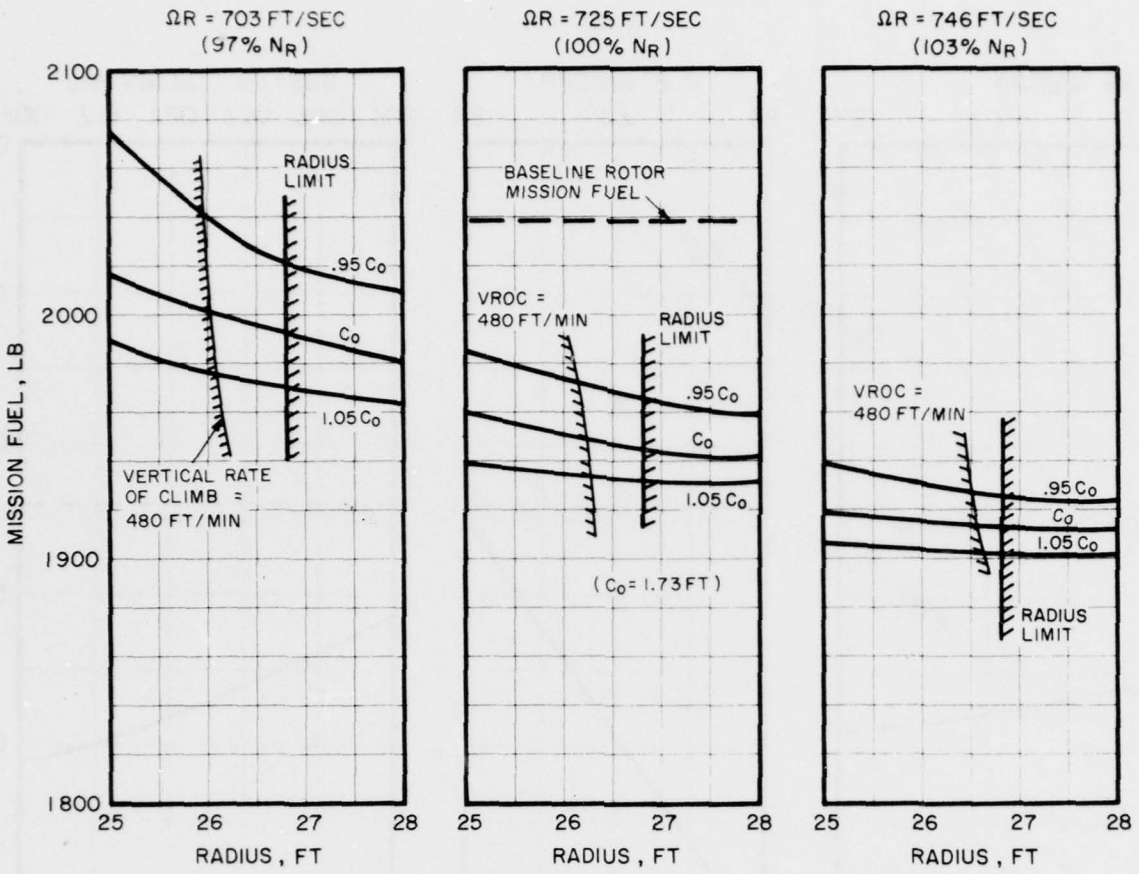

Figure 9. Variation in UH-60A Mission Fuel With Blade Design Changes Assuming a 10 Percent Increase in Cruise L/D and a 2 Percent Increase in Hover Figure of Merit.

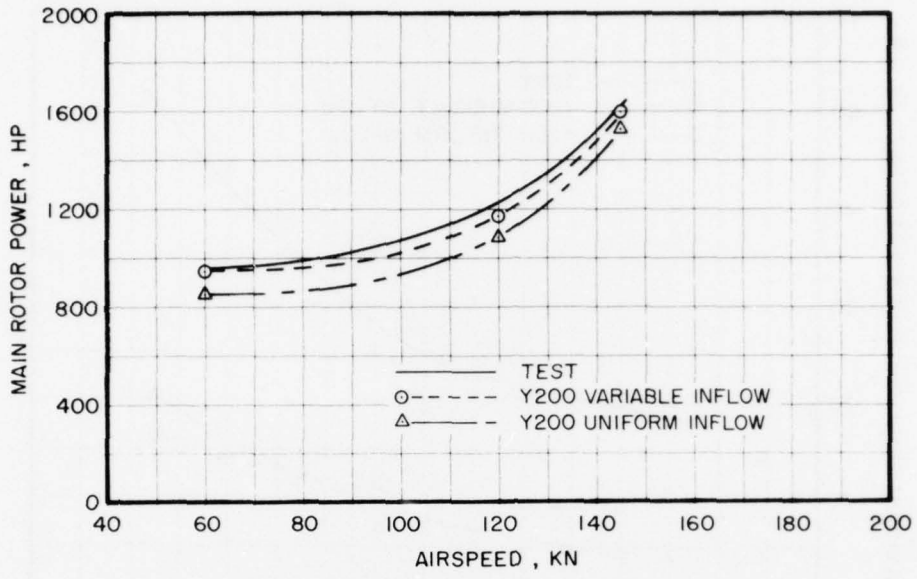

(a)

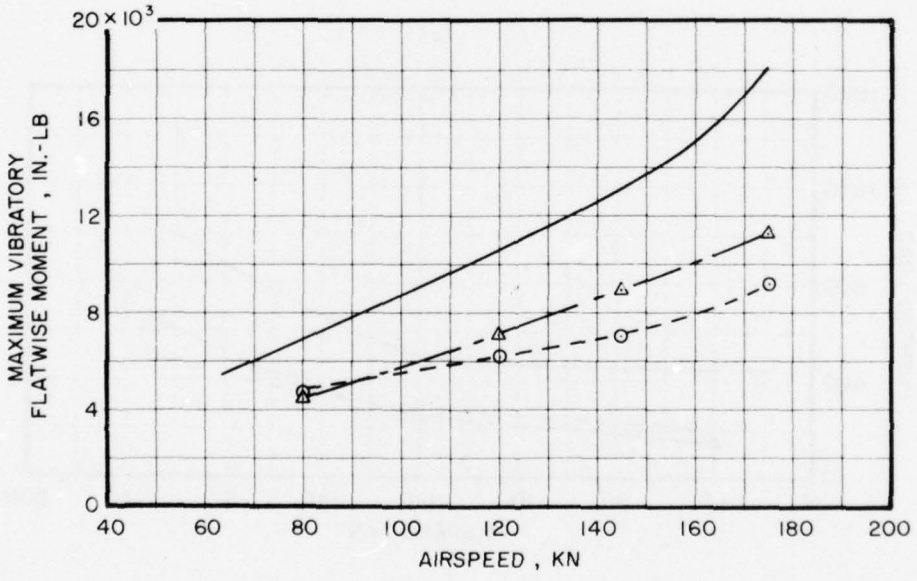

(b)

Figure 10. Correlation of Measured and Predicted YUH-60A Performance and Blade Loads at Approximately 16,450 lb Gross Weight.

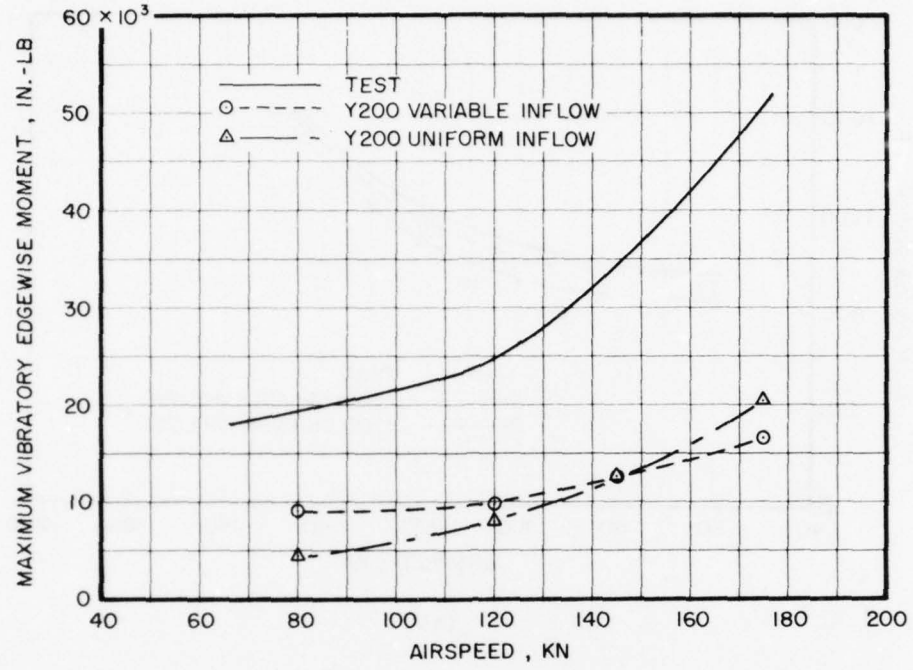

(c)

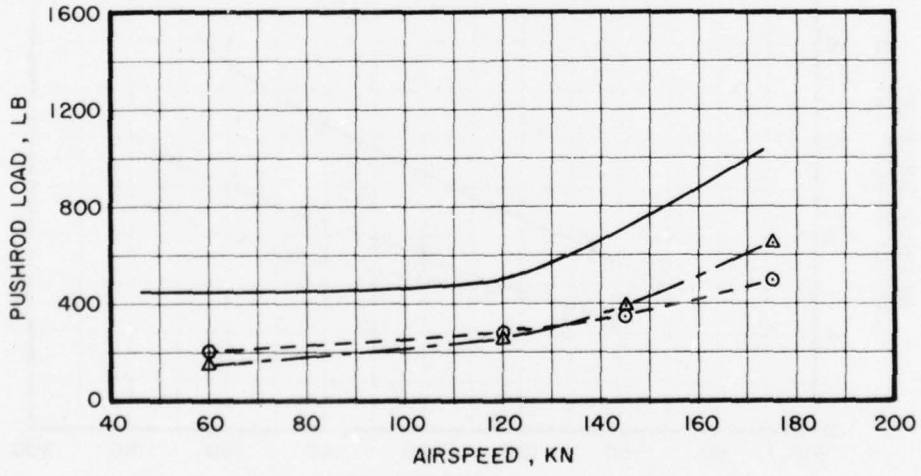

(d)

Figure 10. Concluded.

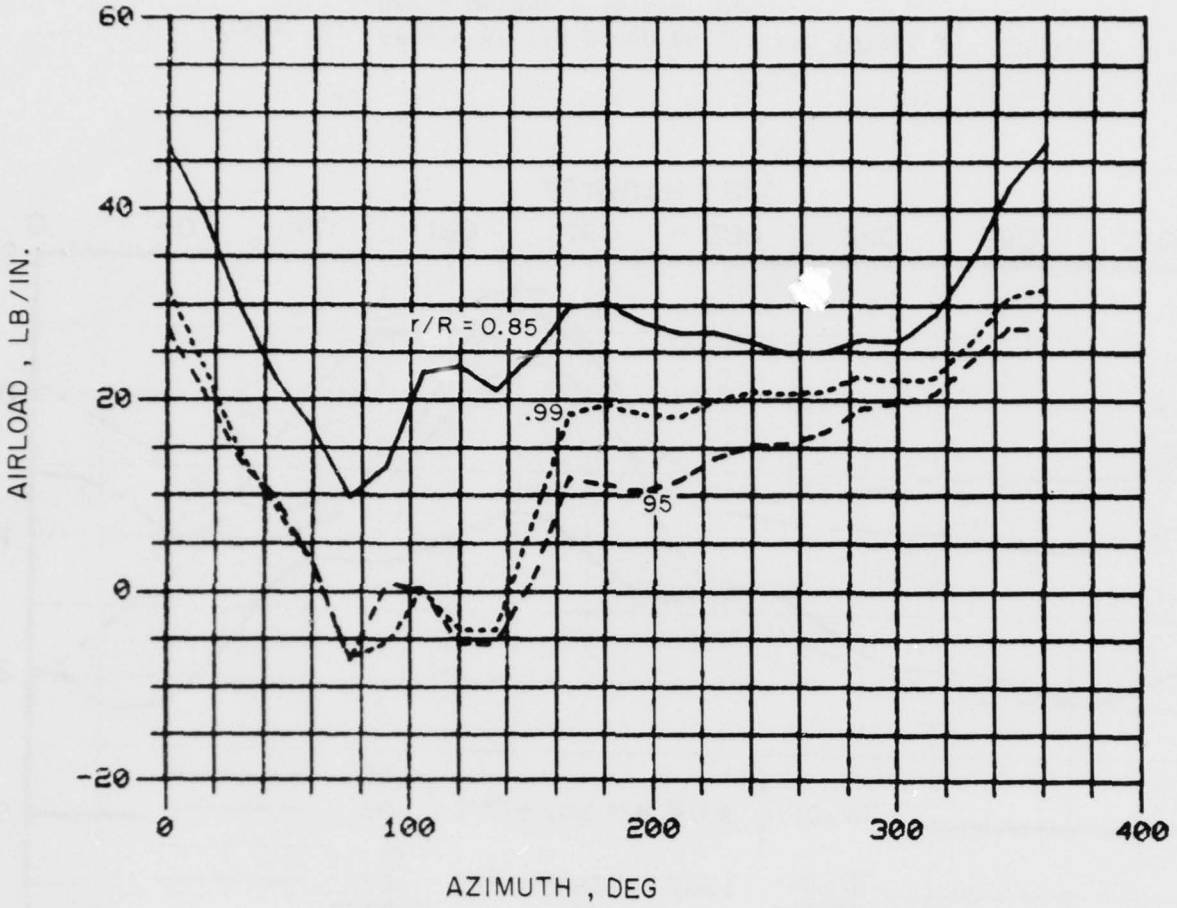

Figure 11. Predicted Airload Time Histories for UH-60 Rotor at Cruise; V = 145 kn, Gross Weight = 16,450 lb.

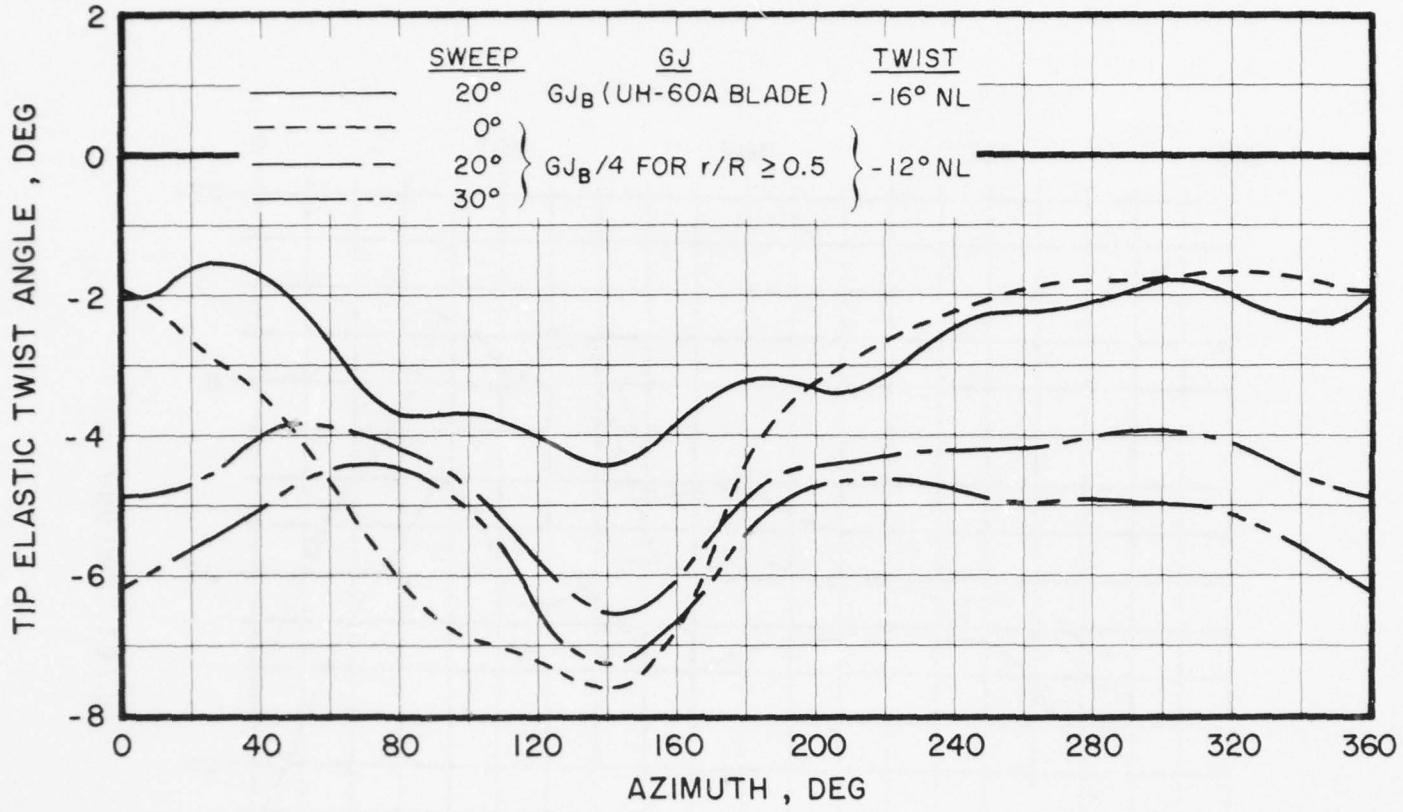

Figure 12. Effect of Tip Sweep on Elastic Twist; V = 145 kn, Gross Weight = 16,450 lb.

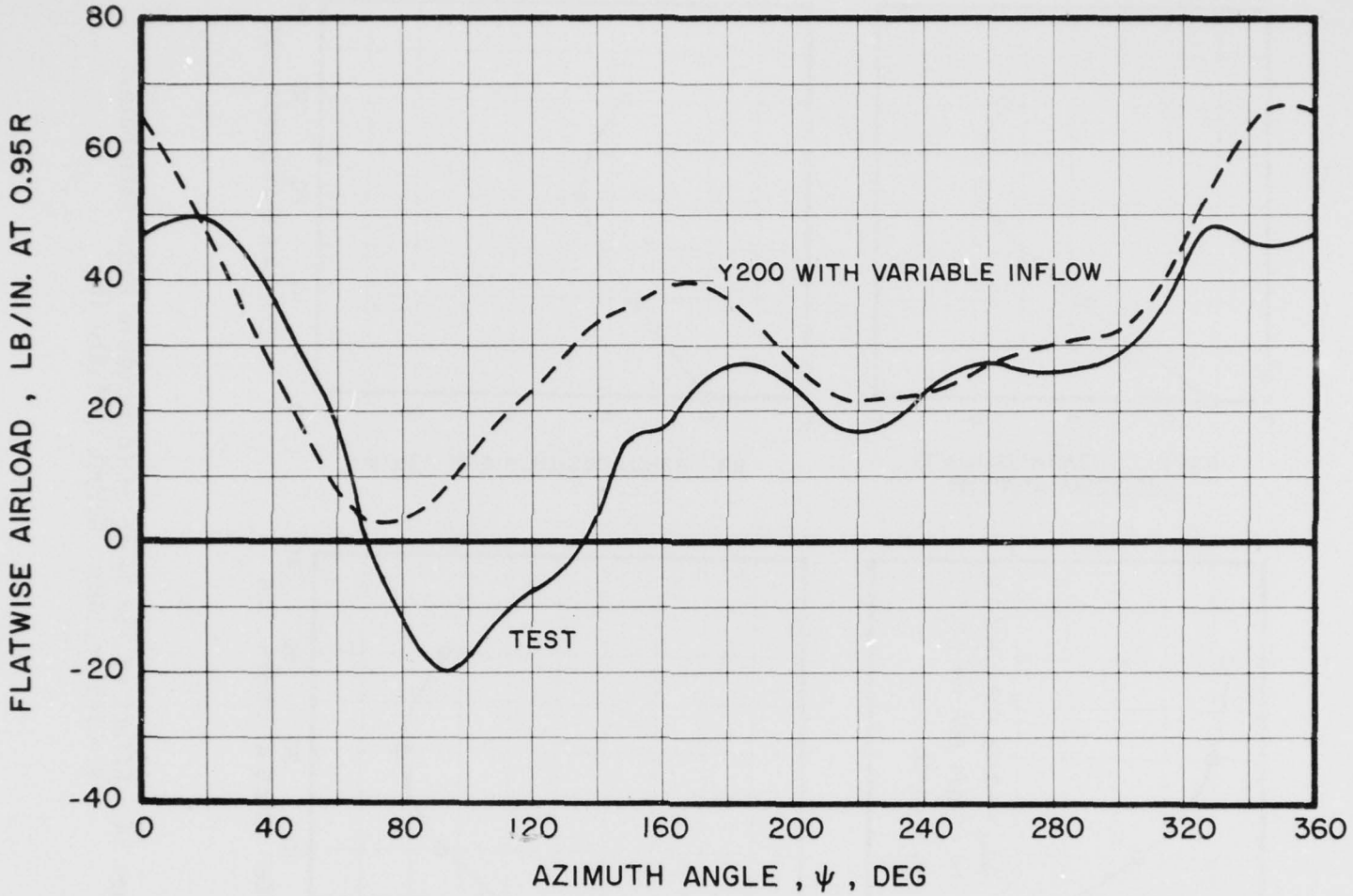

Figure 13. Comparison of Measured and Predicted Airloads for CH-53A Blade; V = 155 kn, Gross Weight = 33,850 lb.

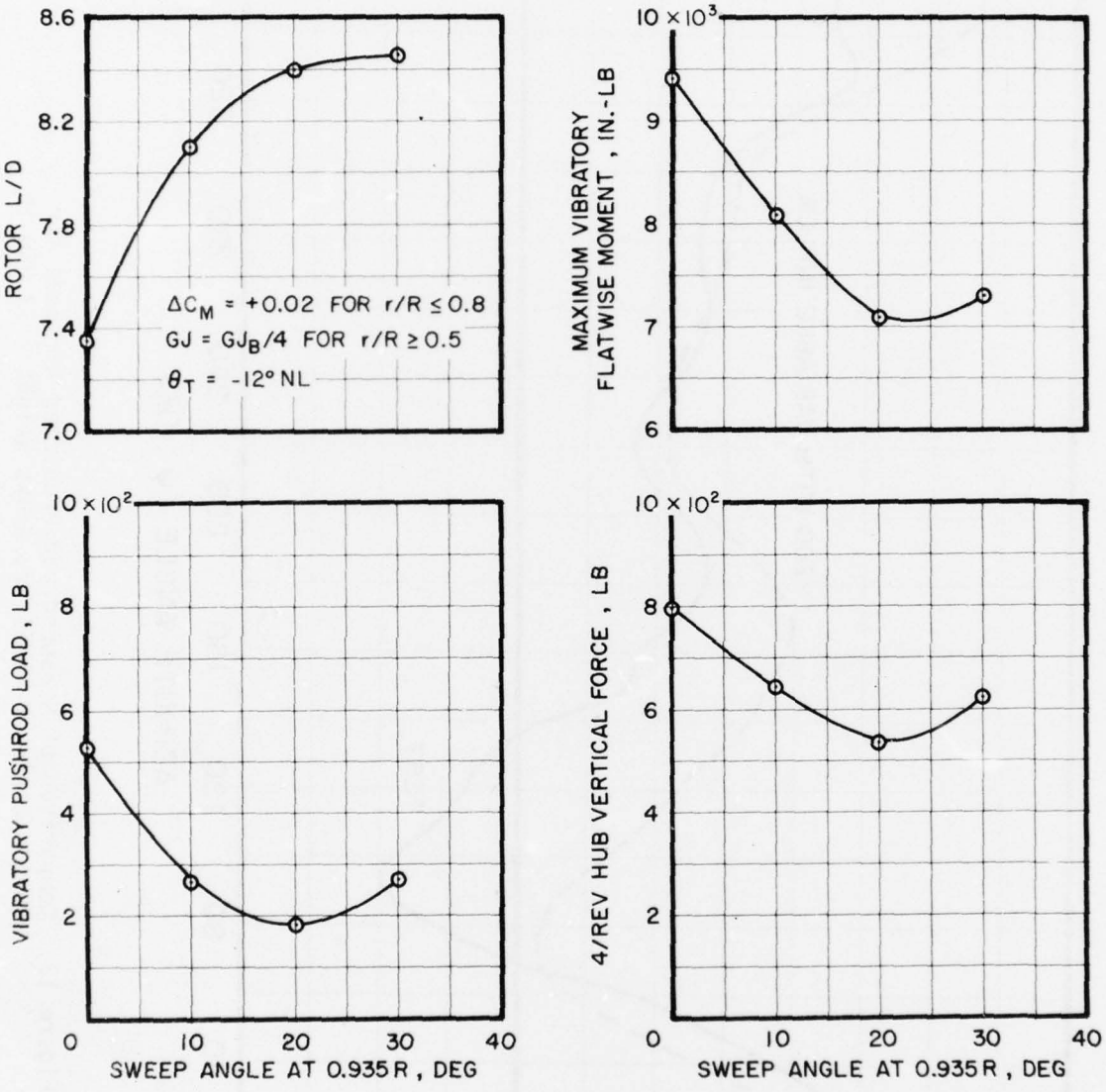

Figure 14. Effect of Tip Sweep on Conformable Rotor Attributes; V = 145 kn, Gross Weight = 16,450 lb.

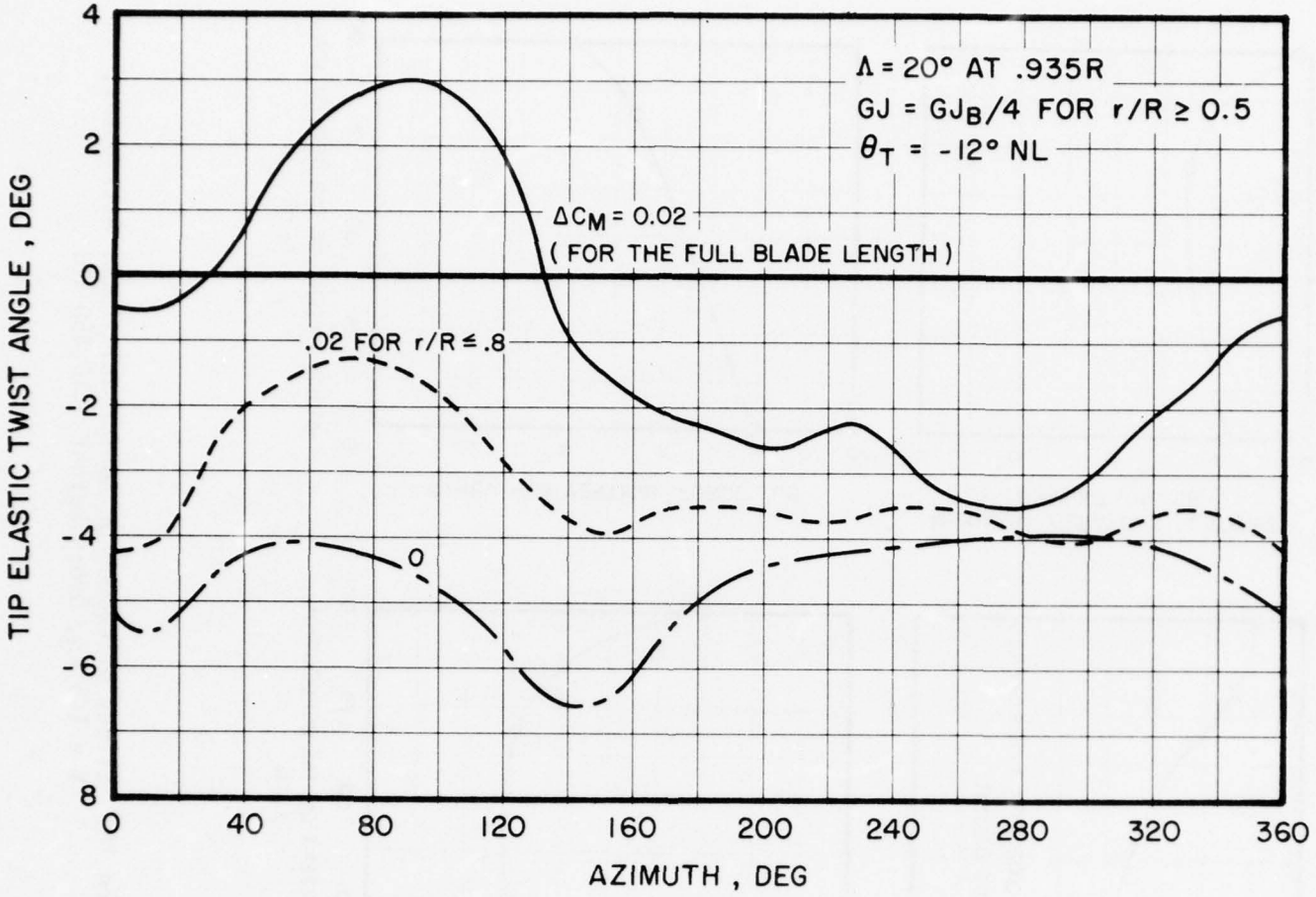

Figure 15. Effect of Camber on Elastic Twist; V = 145 kn, Gross Weight = 16,450 lb.

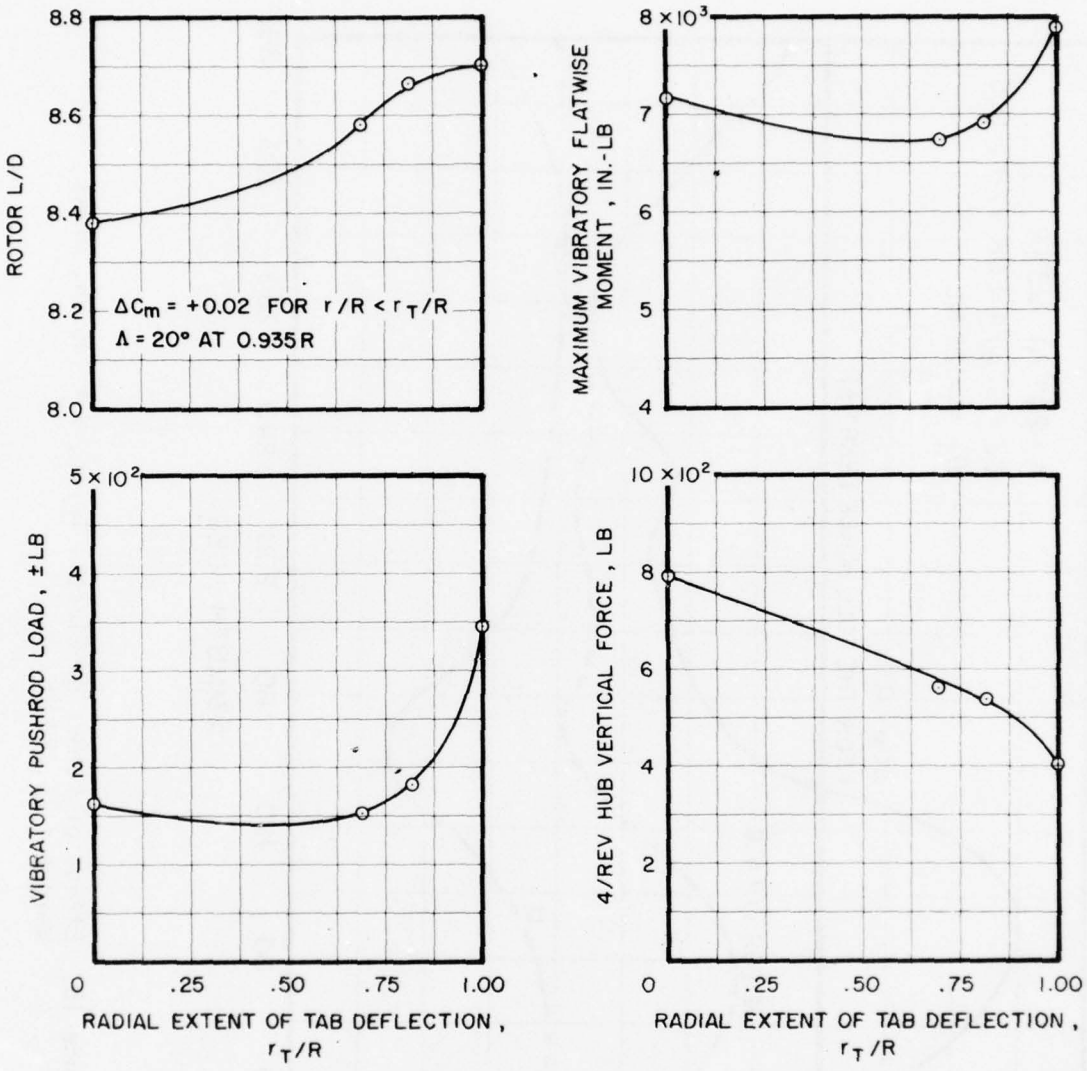

Figure 16. Effect of Camber on Conformable Rotor Attributes; V = 145 kn, Gross Weight = 16,450 lb.

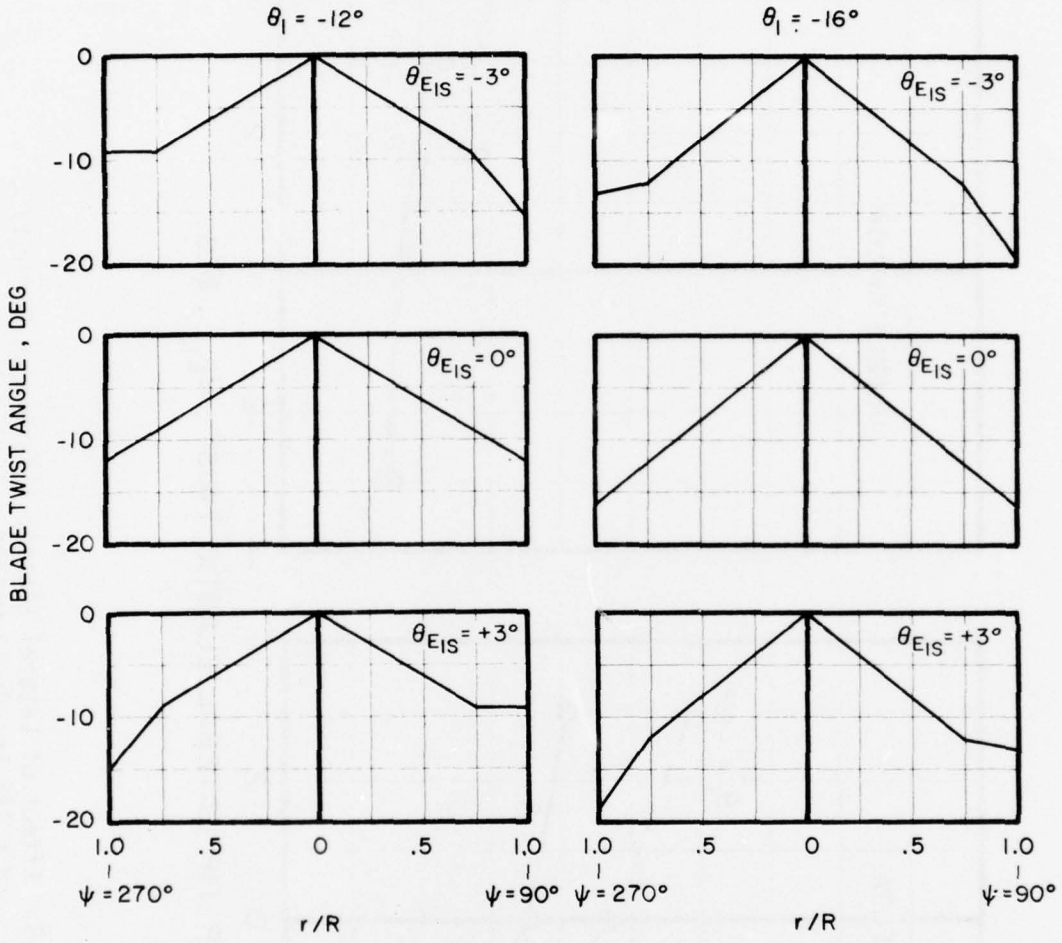

Figure 17. Blade Twist Patterns Examined with the Y200 Program.

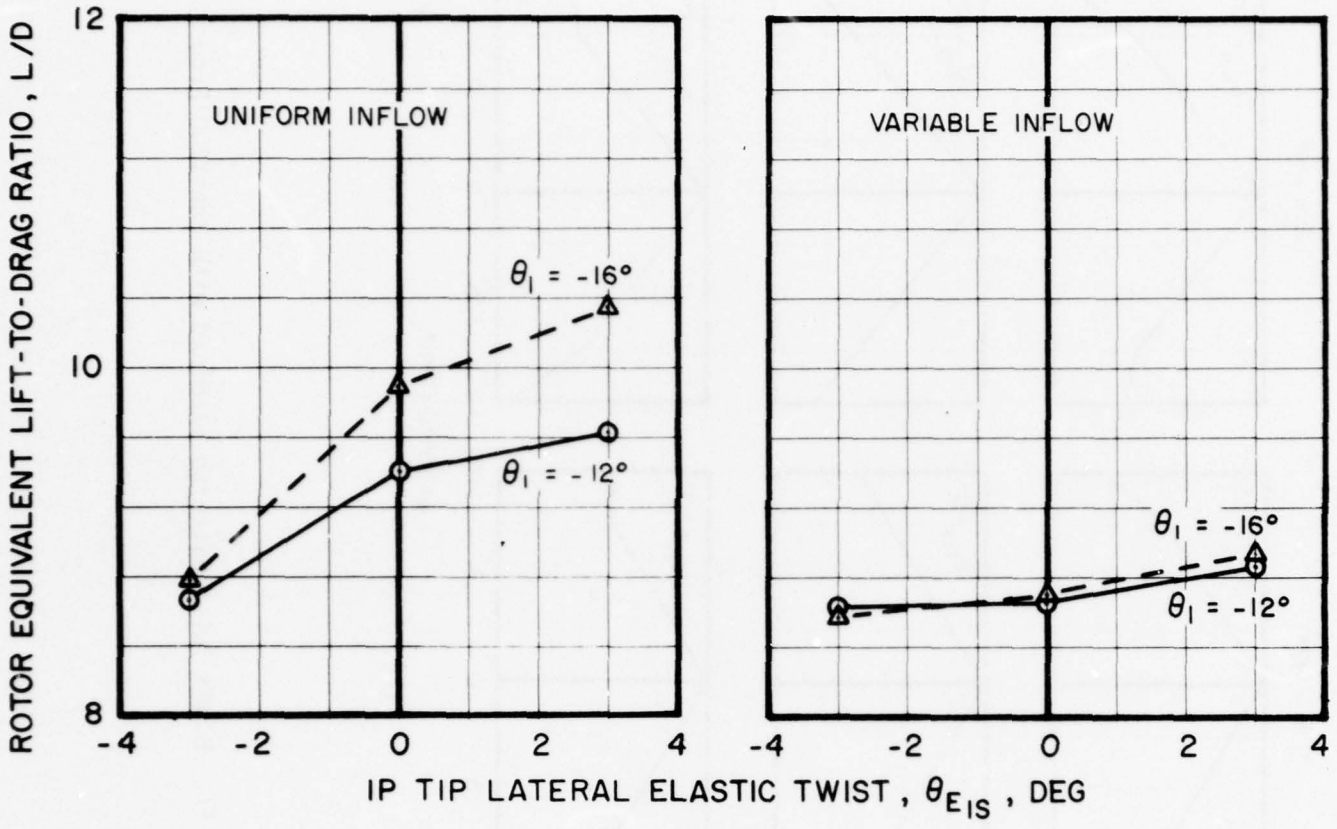

Figure 18. Effect of Lateral Elastic Twisting on Rotor L/D; V = 145 kn, Gross Weight = 16,450 lb.

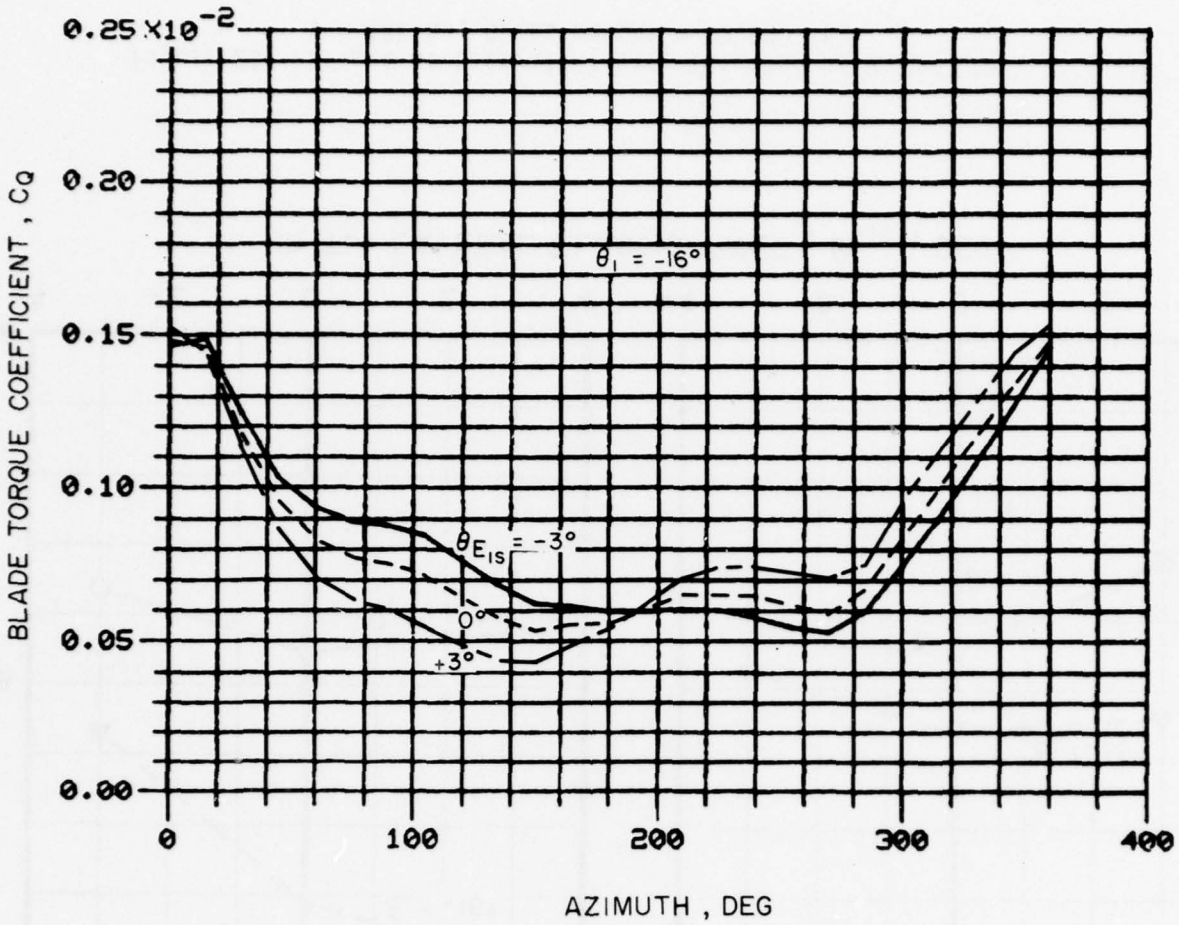

Figure 19. Effect of Lateral Elastic Twisting on Blade Torque Distribution; V = 145 kn, Gross Weight = 16,450 lb.

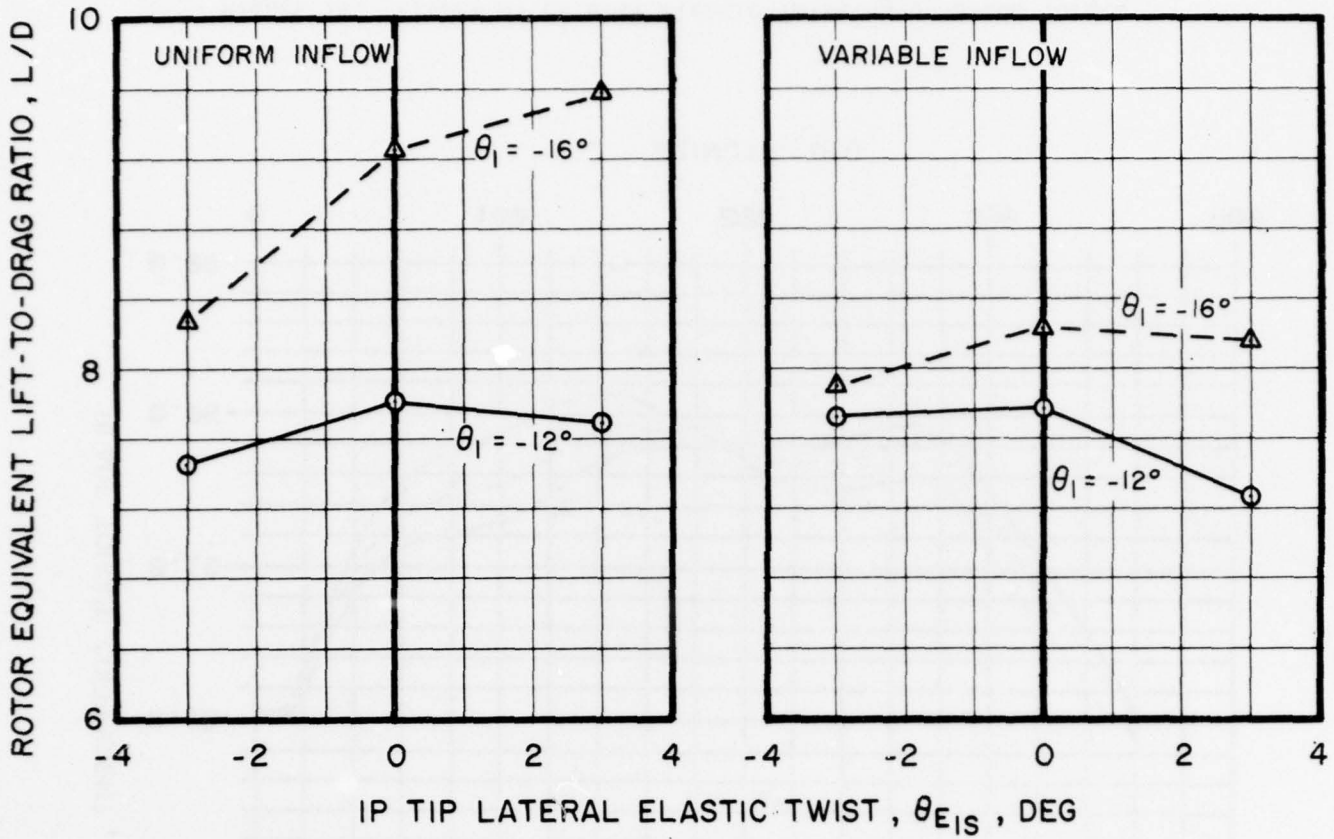

Figure 20. Effect of Lateral Elastic Twisting on Rotor L/D; V = 145 kn, Gross Weight = 19,000 lb.

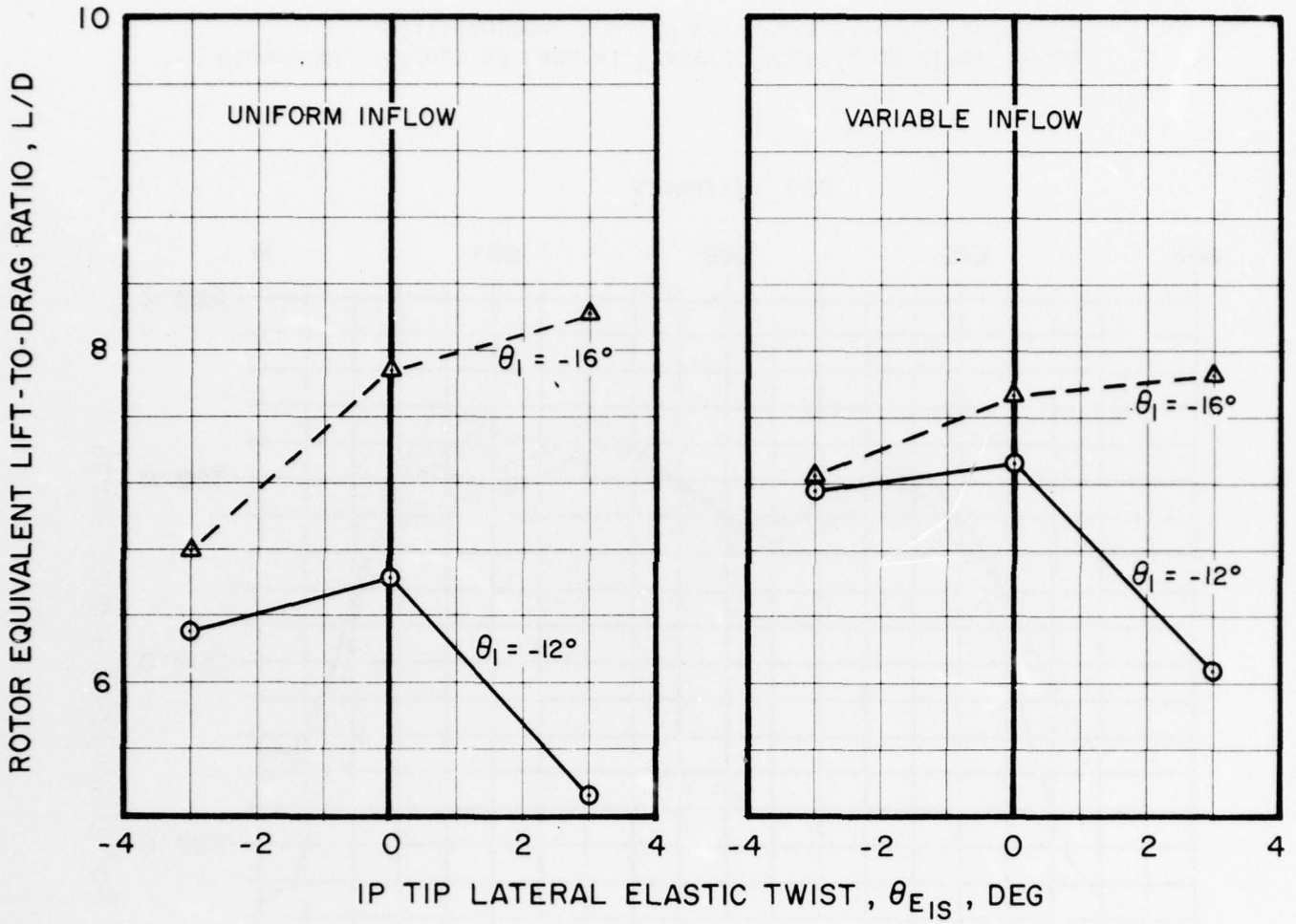

Figure 21. Effect of Lateral Elastic Twisting on Rotor L/D; V = 175 kn, Gross Weight = 16,450 lb.

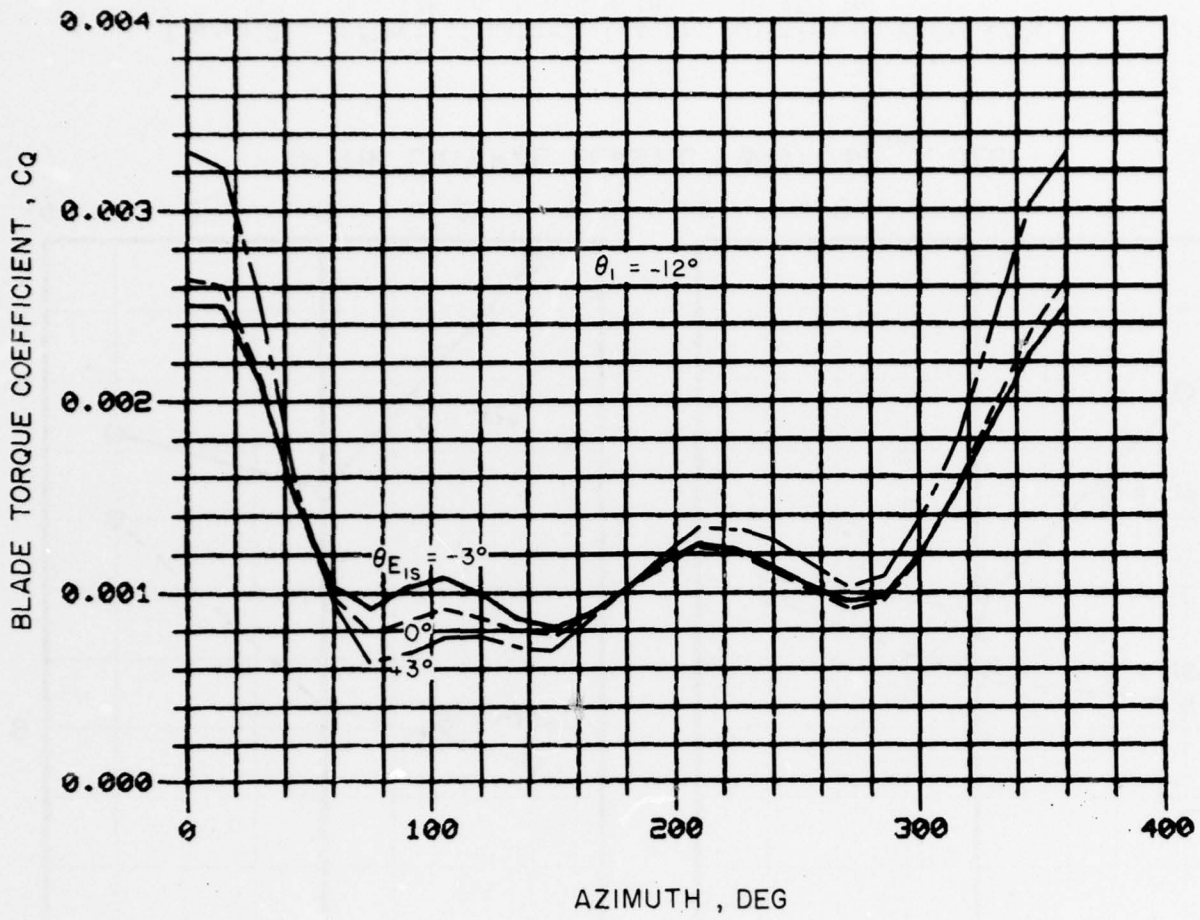

Figure 22. Effect of Lateral Elastic Twisting on Blade Torque Distribution; V = 175 kn, Gross Weight = 16,450 lb.

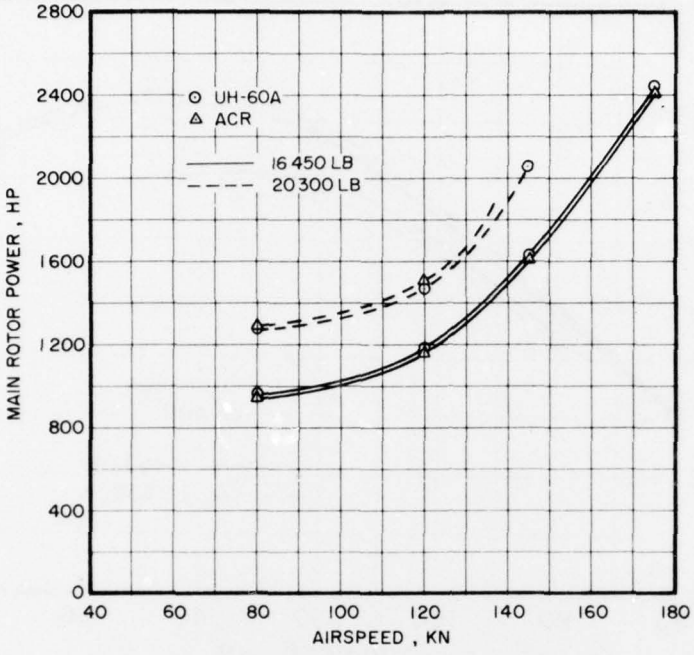

(a)

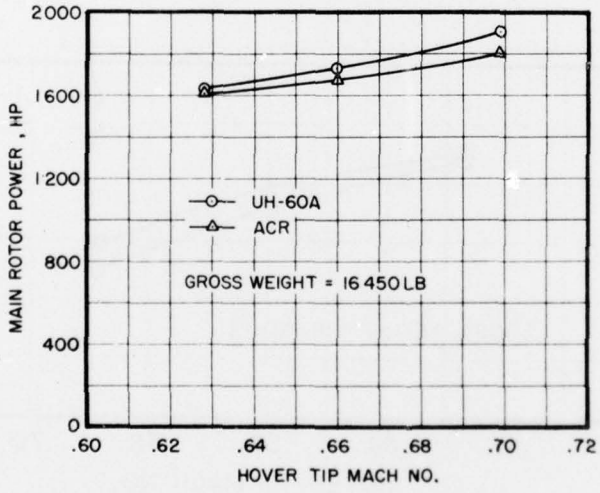

(b)

Figure 23. Comparison of UH-60A and Conformable Rotor Power Required.

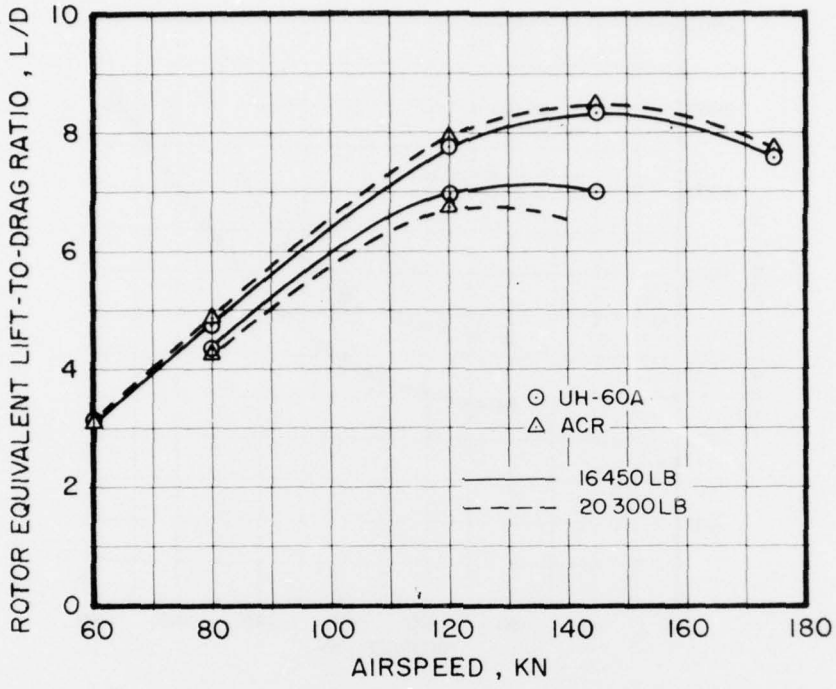

(a)

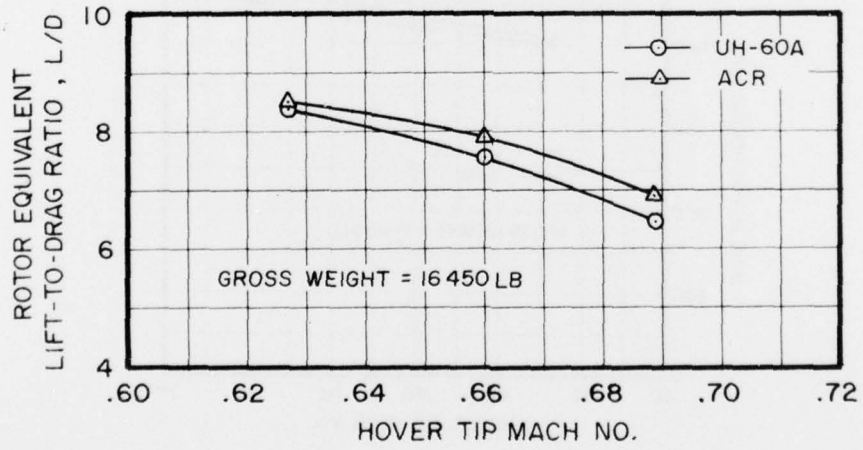

(b)

Figure 24. Comparisons of UH-60A and Conformable Rotor L/D.

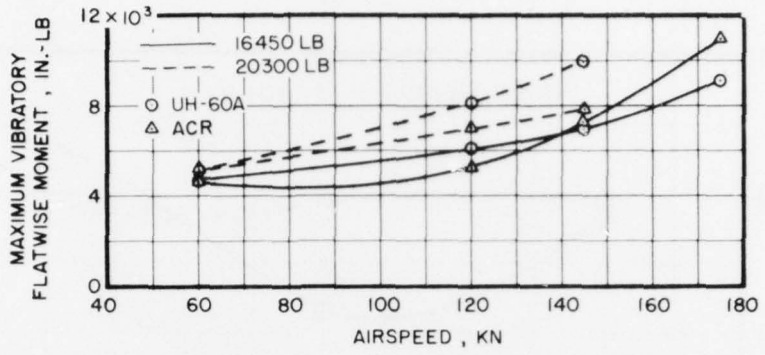

(a)

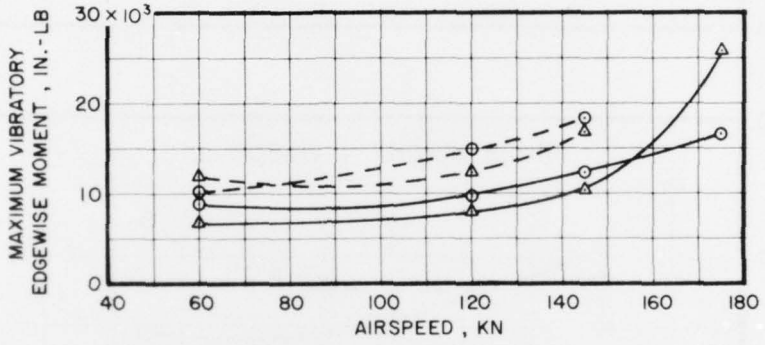

(b)

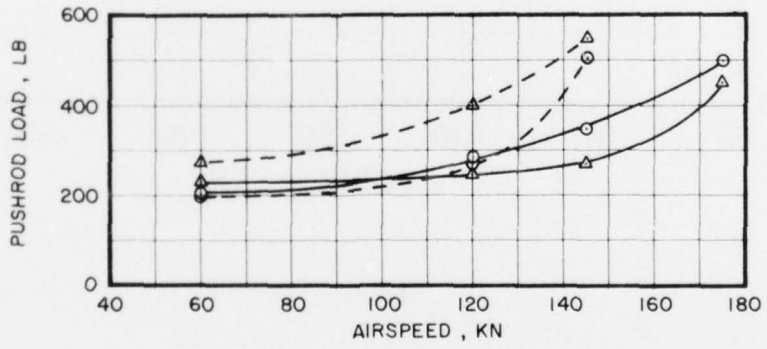

(c)

Figure 25. Comparison of UH-60A and Conformable Rotor Attributes.

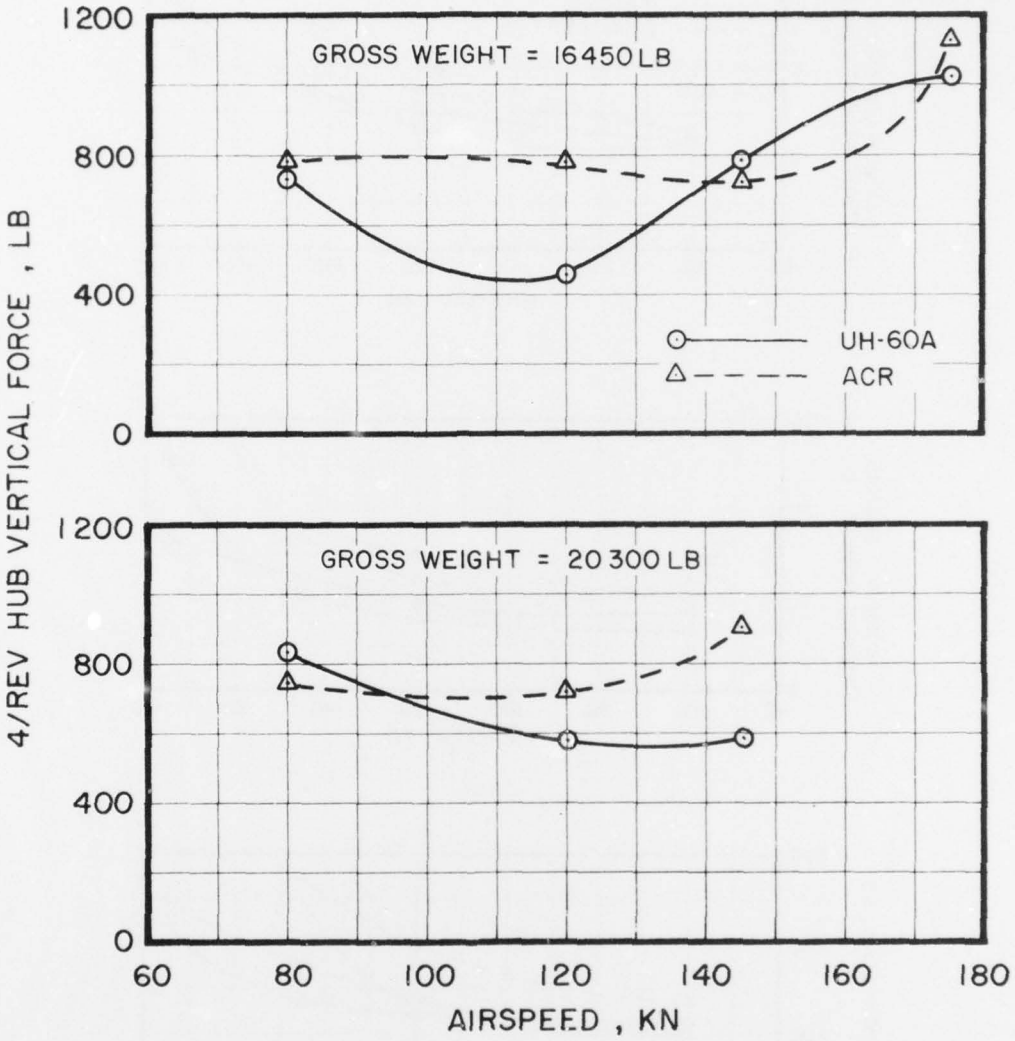

(d)

Figure 25. Concluded.

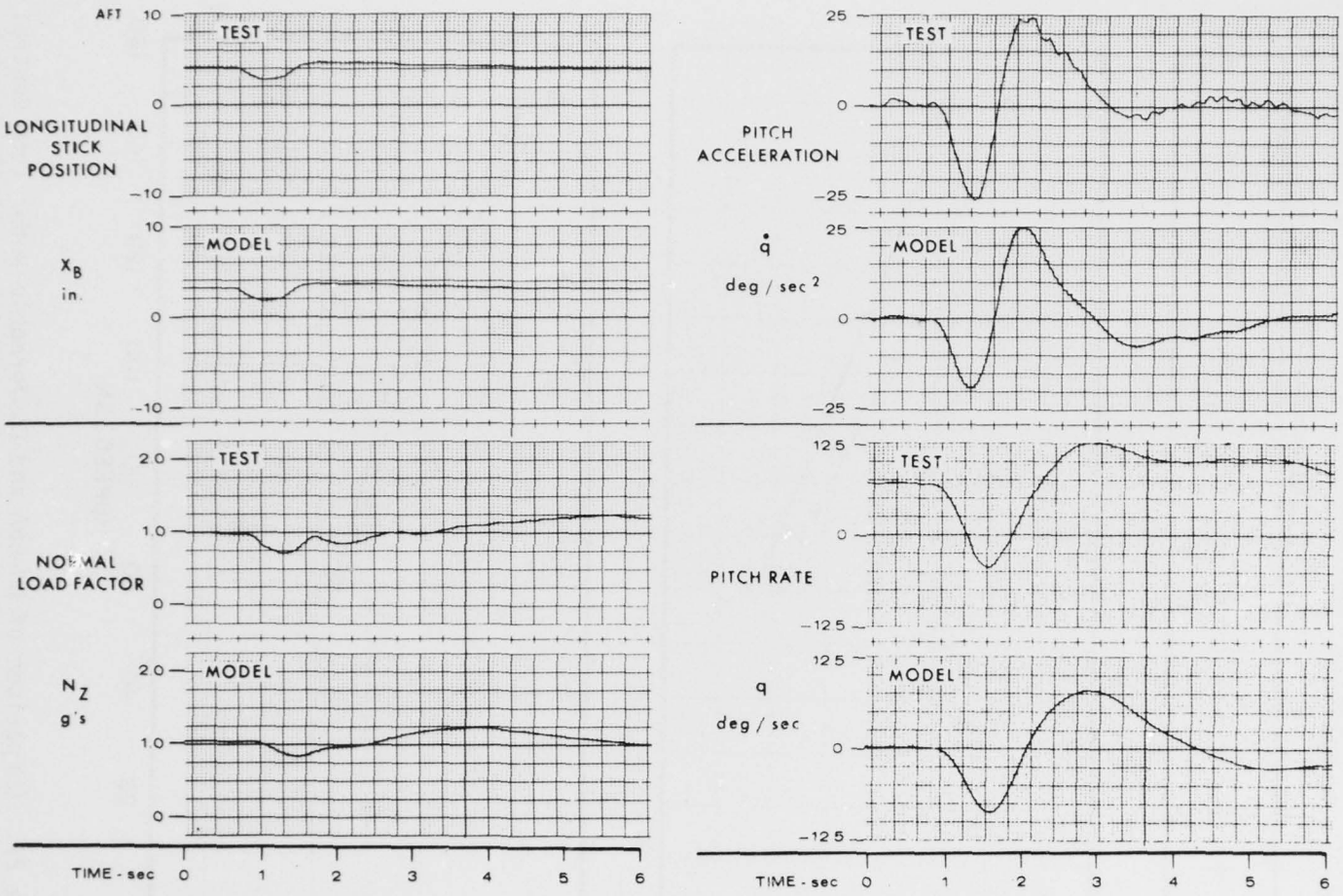

Figure 26. Correlation Between Measured and Calculated Response to Longitudinal Stick Input at 80 kn.

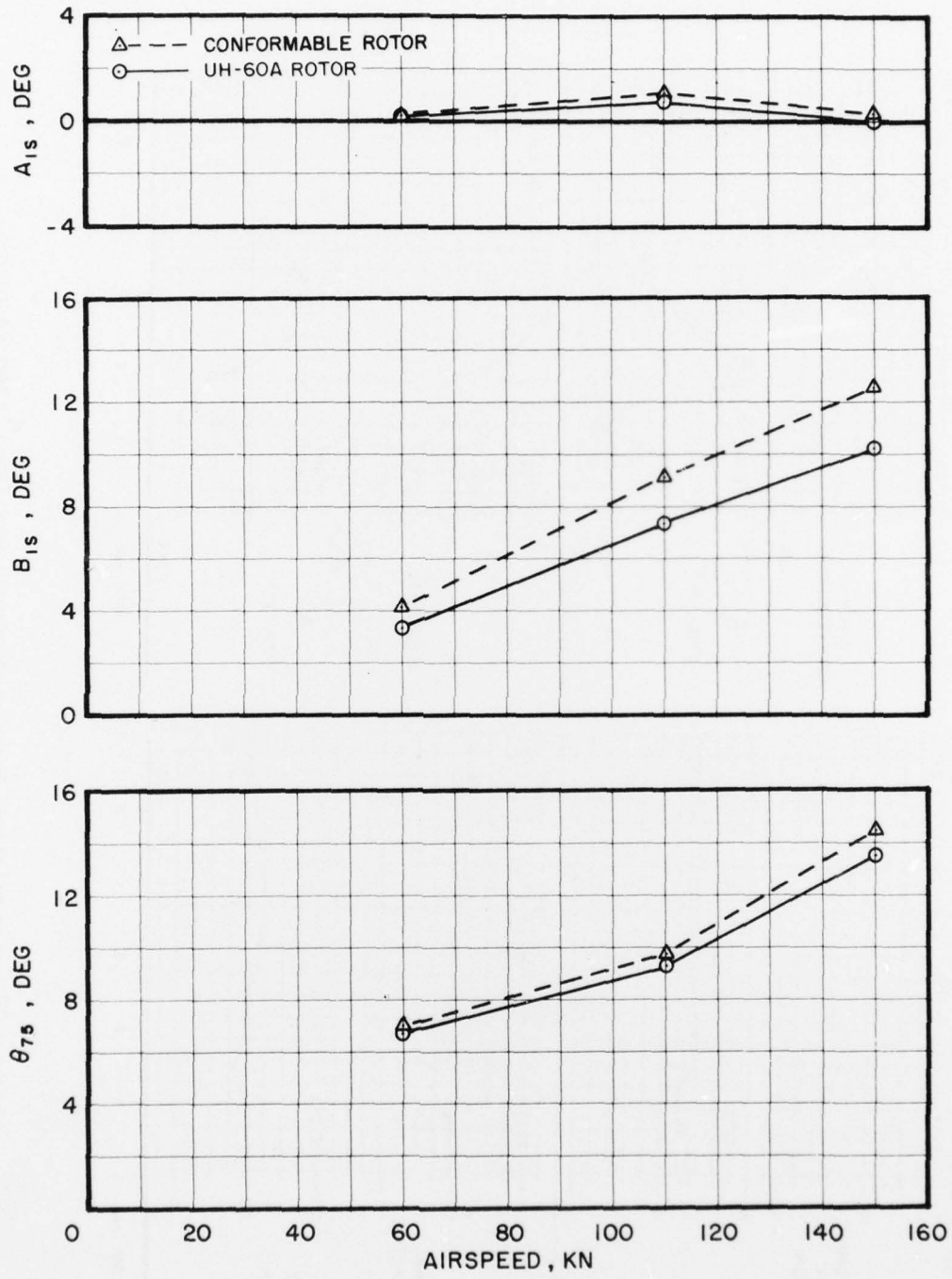

Figure 27. Comparison of UH-60A and Conformable Rotor Trim Control Inputs for Level Flight; Gross Weight = 16,450 lb, Sea Level Standard Conditions.

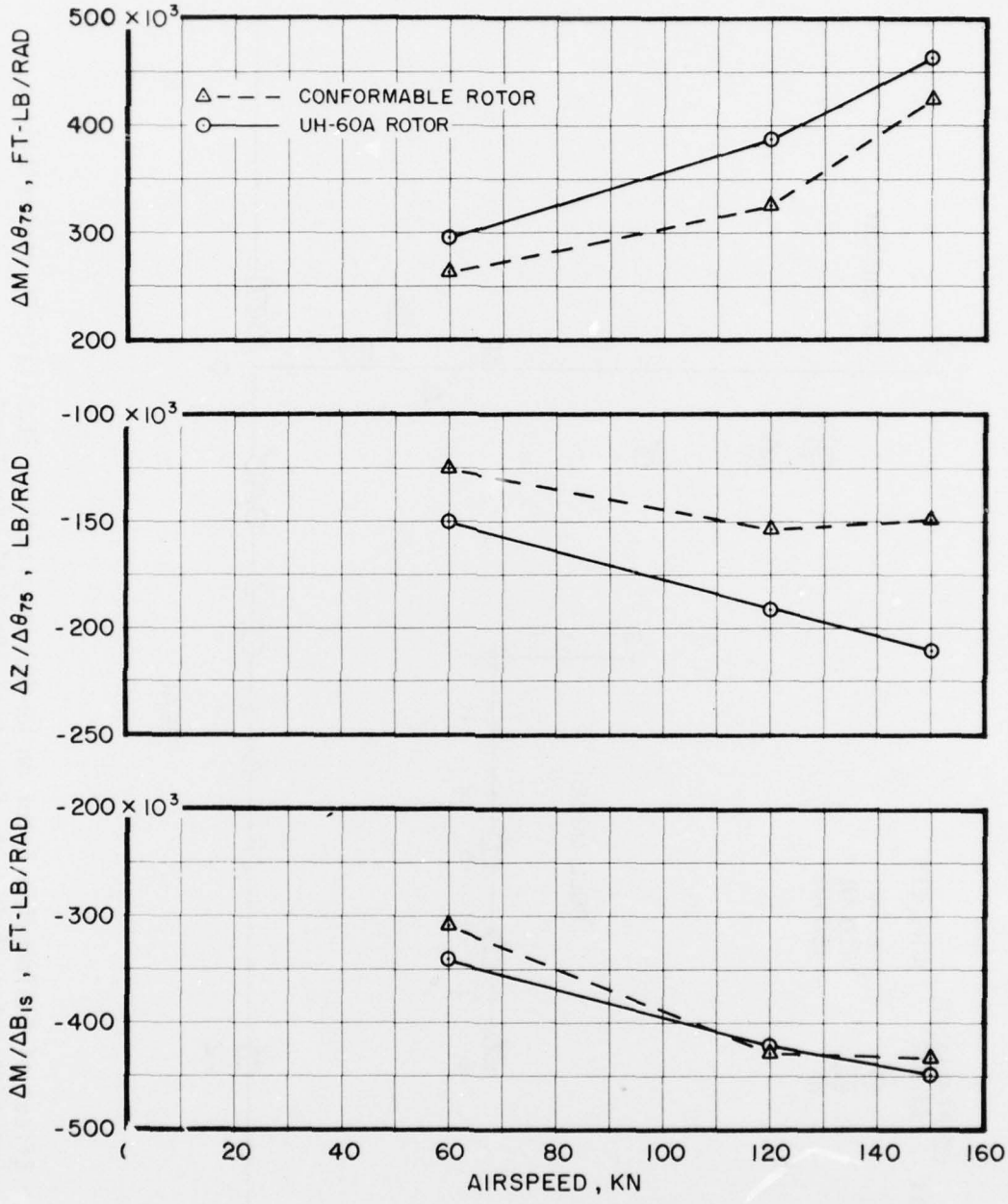

Figure 28. Comparison of UH-60A and Conformable Rotor Control Derivatives; Gross Weight = 16,450 lb, Sea Level Standard Conditions.

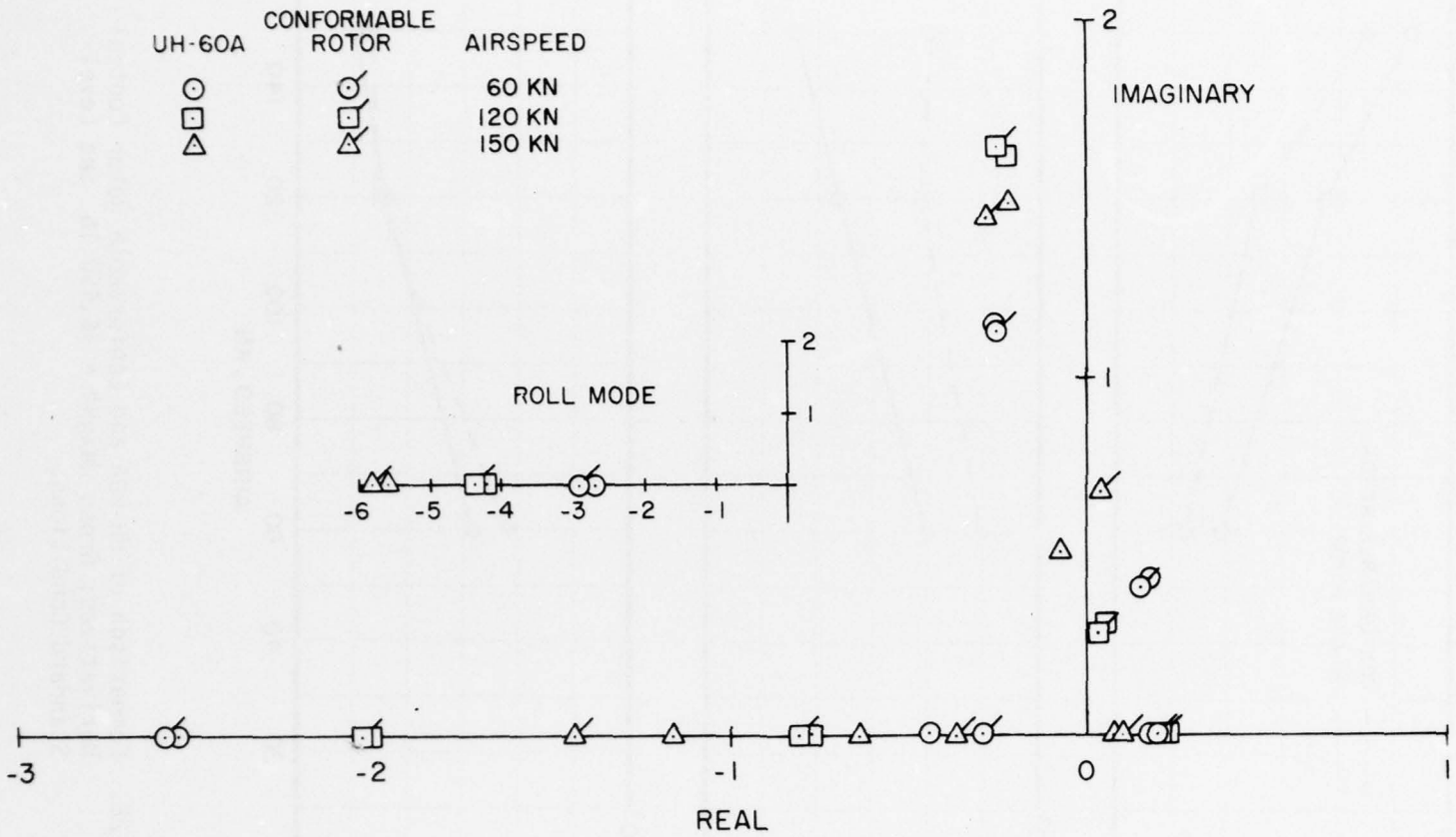

Figure 29. Effect of Conformable Rotor on UH-60A Longitudinal Stability Characteristics; Gross Weight = 16,450 lb, Sea Level Standard Conditions.

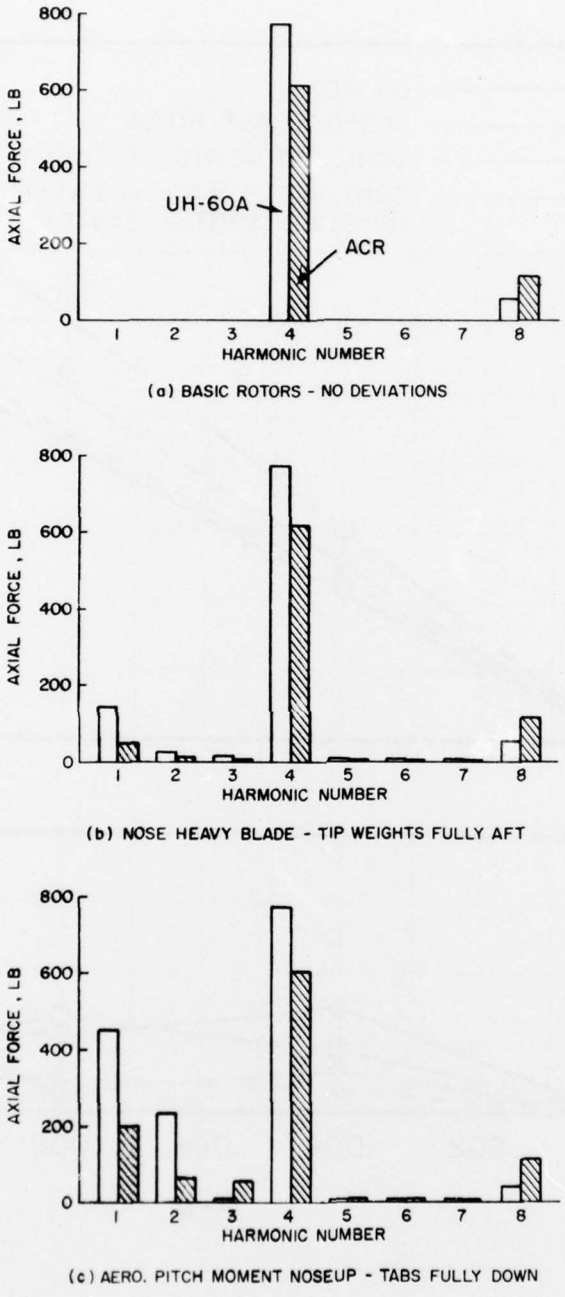

Figure 30. Comparison of Axial Hub Force Components for UH-60A and Conformable Rotor Blade Sets with Manufacturing Deviations; V = 145 kn, Gross Weight = 16,450 lb.

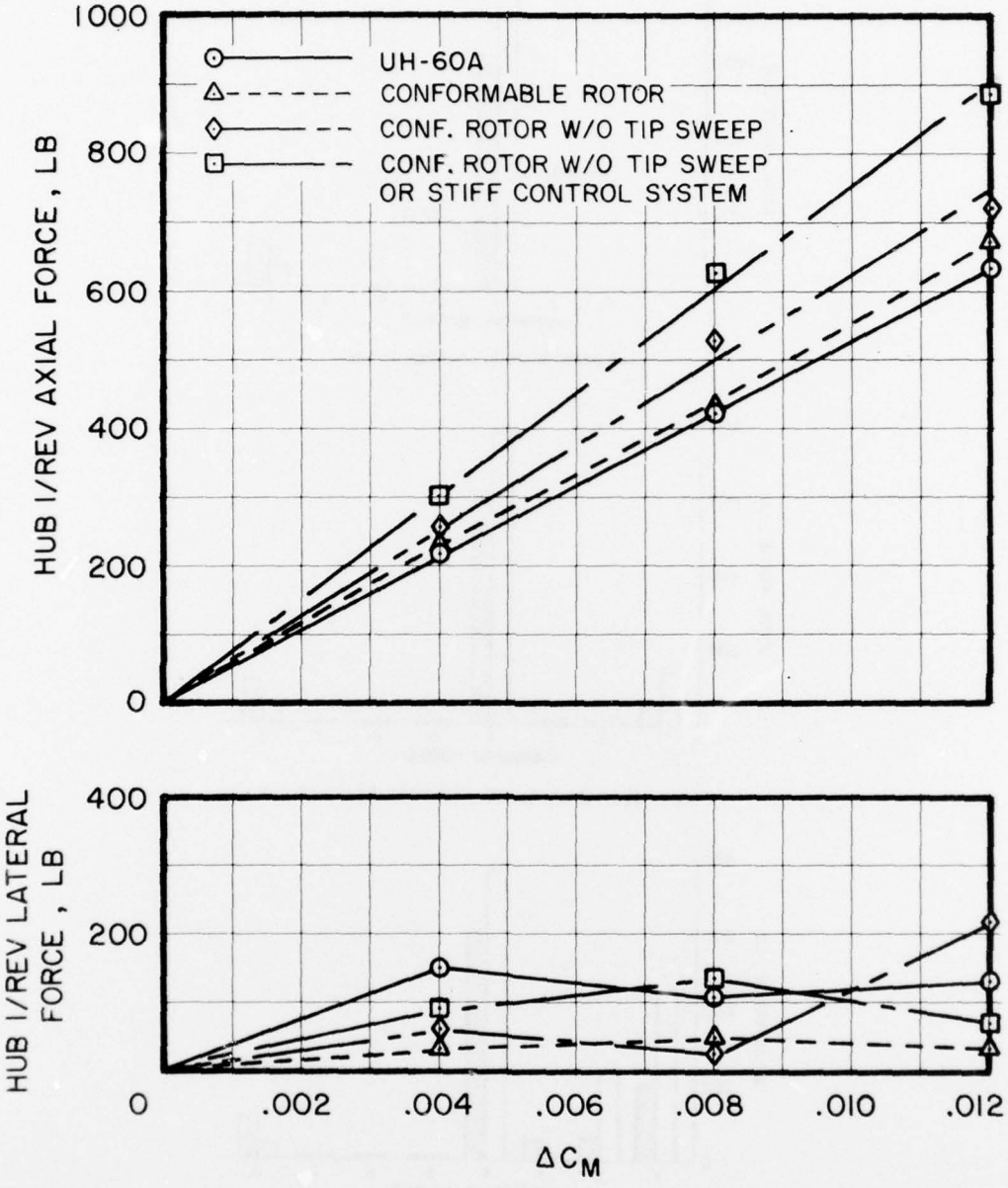

Figure 31. Comparison of One/Rev Hub Forces for Damaged UH-60A and Conformable Rotor Blade Sets; V = 145 kn, Gross Weight = 16,450 lb.

LIST OF SYMBOLS

A_{1s}	Lateral cyclic pitch, positive for increased pitch at 180 deg azimuth, deg
B_{1s}	Longitudinal cyclic pitch, positive for increased pitch at 270 deg azimuth, deg
c	Blade chord, ft
C_L	Rotor lift coefficient, $L/\pi R^2\rho(\Omega R)^2 R$
c_m	Section pitching moment coefficient
C_T	Rotor thrust coefficient, $T/\pi R^2\rho(\Omega R)^2$
C_Q	Rotor torque coefficient, $Q/\pi R^2\rho(\Omega R)^2 R$
c_Q'	Blade torque coefficient, $2Q'/R^2\rho(\Omega R)^2 R$
D	Rotor equivalent drag, $\frac{550}{V}$ (HP - HP_{PAR}), lb
FM	Figure of merit, $\frac{1}{\sqrt{2}} \frac{C_T^{3/2}}{C_Q}$
GJ	Blade torsional stiffness
h_p	Pressure altitude, ft
HP	Horsepower
HP_{PAR}	Parasite horsepower
L	Rotor lift, lb
M	Aircraft pitching moment, positive for noseup moment, ft-lb
N_Z	Aircraft load factor
q	Pitch rate, positive for noseup motion, deg/sec
Q	Rotor torque, ft-lb
Q'	Instantaneous blade torque, ft-lb
r	Blade radial coordinate, ft
R	Blade radius, ft
T	Rotor thrust, lb
V	Airspeed, kn

v_x	Longitudinal component of aircraft velocity in body axis system, positive forward, ft/sec
v_z	Component of aircraft velocity parallel to shaft, positive down, ft/sec
x_B	Longitudinal stick position, positive aft, in
W_b	Blade weight, lb
Z	Component of total rotor force parallel to shaft, positive down, lb
Δc_m	Change in section pitching moment coefficient due to camber
θ_1	Blade linear twist, deg
θ_{75}	Blade pitch angle at three-quarter radius, deg
$\theta_{E_{ls}}$	Lateral component of one-per-rev tip elastic twist, positive for noseup advancing blade twist, deg
θ_T	Total blade twist, deg
Λ	Tip sweep angle, positive aft, deg
μ	Advance ratio
ρ	Density of air, slug/ft^3
σ	Rotor solidity
ψ	Blade azimuth position, positive counterclockwise referenced to downstream position, deg
Ω	Rotor rotational speed, rad/sec
1P	First harmonic of rotor rotational frequency

1733-79